Fusion—Reactor Materials

A Litnovsky[a,b], I Duran[c], JW Coenen[a,d], Yu Gasparyan[b], MR Gilbert[e], E Hollmann[f], Ch Linsmeier[a], S Nogami[g], CH Skinner[h], and S Zinkle[i], [a]Forschungszentrum Jülich GmbH, Institut für Energie- und Klimaforschung, Jülich, Germany; [b]National Research Nuclear University MEPhI, Moscow, Russian Federation; [c]Institute of Plasma Physics of the Czech Academy of Sciences, Praha, Czech Republic; [d]Department of Engineering Physics, University of Wisconsin Madison, Madison, WI, United States; [e]United Kingdom Atomic Energy Authority, Culham Science Centre, Abingdon, Oxfordshire, United Kingdom; [f]University of California–San Diego, La Jolla, CA, United States; [g]Department of Quantum Science & Energy Engineering, Graduate School of Engineering, Tohoku University, Sendai, Japan; [h]Princeton Plasma Physics Laboratory, Princeton, NJ, United States; [i]University of Tennessee, Knoxville, TN, United States

Introduction

The aim of controlled fusion is to produce electricity from the energy released by fusion reactions with a competitive cost efficiency, maximum safety and with least environmental impact. In order for nuclear reactions to become effective, the fusion particles of relevant energies in keV range must be brought together at sufficient concentration for sufficient time defined by Lawson criterion (Lawson, 1957), as discussed in detail in Wade (2021). The Lawson criterion defines the condition, at which the energy balance is positive by comparing the energy released in fusion reactions to the energy lost to the environment. Quantitatively, for deuterium (D) and tritium (T) reaction, assuming 50%–50% mixture and temperature above 10 keV (1.16×10^8 K), the Lawson criterion can be written as:

$$n\tau_E > 10^{20}\ \mathrm{s} \times \mathrm{m}^{-3}, \tag{1}$$

where n is the number density of reacting particles and τ_E is the energy confinement time. From the formula (1) we may see that there are two possible ways to attain the positive balance of energy gained from fusion compared to energy loses:

1. by increasing the confinement time at the given density of reacting particles;
   or
2. by increasing the density of reacting particles possibly, interacting within the very short time.

These fundamentally different approaches have led to two main technological concepts in realizing the controlled production of nuclear fusion energy: magnetic confinement concept and inertial confinement concept.

In magnetic confinement fusion (MCF) devices, such as tokamaks (Artsimovich, 1972; Wesson and Campbell, 2011), described in detail by Zohm (2021) and stellarators (Spitzer et al., 1954), discussed by Yamada (2021) and relatively rarely, magnetic traps (Ioffe, 1965). The long-pulse or quasi-stationary fusion plasmas are confined in the vacuum vessel by a strong magnetic field. In tokamaks and stellarators, such a magnetic field is created using the external coils surrounding a donut-shaped vacuum vessel. The variety of magnetic configurations is discussed in detail by Galvao (2021).

Inertial fusion (IFE) relies on the exposure of deuterium—tritium targets, implosively compressed and heated by intensive laser or ion beams. In the IFE devices, plasma is free to expand after the implosion of the D-T target. More details on inertial fusion concepts and underlying physics can be found e.g. in Norreys (2021) and in Atzeni (2021).

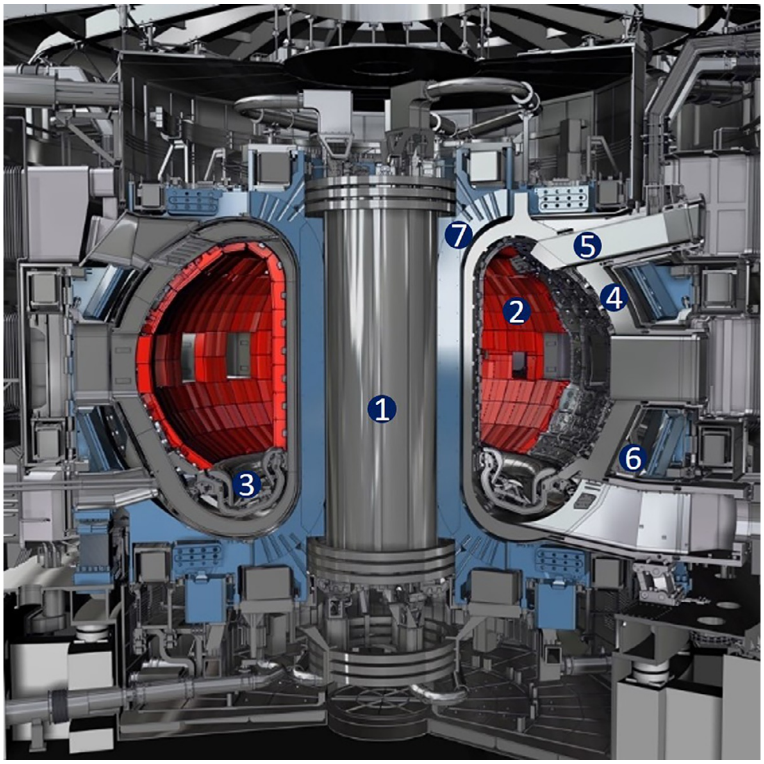

Fig. 1 Main components of the MCF device: (1) central solenoid, (2) plasma-facing first wall, (3) divertor, (4) blanket, (5) one of diagnostic ports, (6) inner infrastructure and (7) magnetic coil. Figure courtesy of ITER Organization.

In both concepts, MCF and IFE, fluxes of fusion plasma particles and intensive radiation come into contact with materials of fusion device. Depending on their function, several material classes are used in the components of the fusion facility illustrated schematically in Fig. 1:

Plasma-facing materials. These materials are exposed to plasma particle and radiation fluxes directly. The role of these materials is to protect the inner structure of the fusion device and to guarantee the low level of plasma impurities in the plasma.

Blanket materials. These materials are located behind the plasma-facing materials. Their main role is to ensure tritium breeding needed for "refilling" the fusion plasma with tritium and to conduct the heat generated by the products of fusion reaction to the coolant—in order to produce electricity from it later.

Diagnostic materials. These materials are used for multiple measurement (i.e. diagnostic) systems of a fusion device. The main role of diagnostic materials is to transfer the information: electromagnetic radiation (e.g. light) from the main fusion plasma towards the corresponding detectors and sensors.

Materials for magnets. These materials are used in the main field magnets and in various magnetic subsystems needed for plasma confinement, positioning and stabilization and for distribution of plasma loads.

Structural materials. The role of these materials is to support the entire first wall, blanket, diagnostic infrastructure and magnets in the most robust and reliable manner. Structural materials are also used to provide the required vacuum conditions in the fusion facility. These materials have to preserve the entire infrastructure integrity under challenging pressure, temperature and seismological conditions.

Magnetic confinement fusion devices

Edge plasma and scrape-off layer

In magnetic confinement fusion devices, in most of the volume occupied by the plasma, the trajectories of plasma particles never intersect the wall of plasma vessel, creating the so-called confined plasma volume, as illustrated in Fig. 2. The total plasma thermal energy accumulated in the central, core confined plasma in a modern tokamak such as ITER (ITER Fusion Reactor Website, 2020) can be as high as several hundreds of megajoules (MJ) (Shimada et al., 2007), whereas in a fusion power plant thermal energy is expected to be of order of one gigajoule (GJ) (Federici et al., 2017, 2018). To confine large accumulated energy, magnetic fields with strengths of several Tesla are used in modern magnetic confinement fusion devices. However, complete confinement cannot be achieved even with the most modern magnet technology.

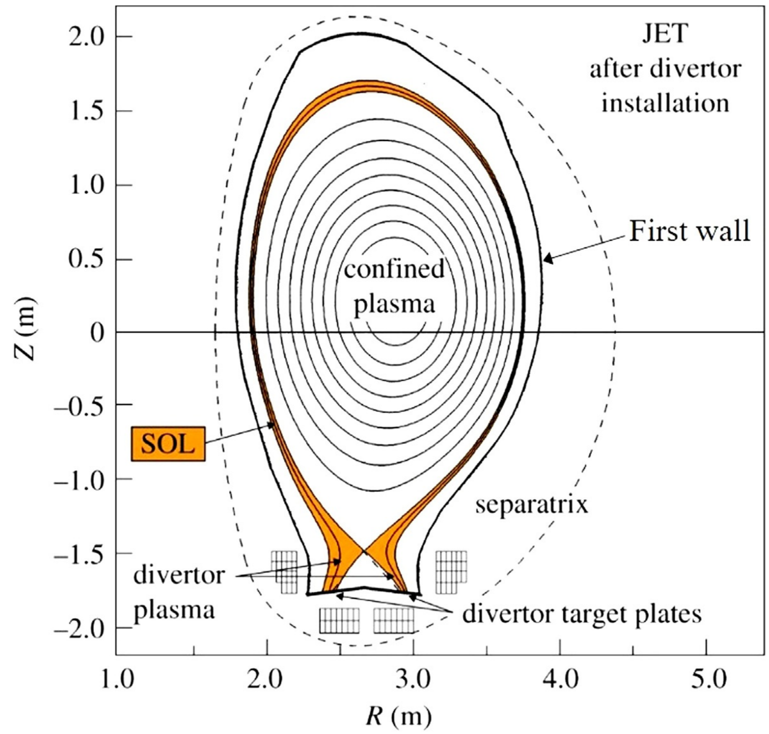

Fig. 2 Main areas occupied by fusion plasmas in a magnetic fusion device: a cross-section of JET tokamak with outlined scrape-off layer (SOL) in between the main confined plasma and the first wall. Adapted from Costley AE (2019) Towards a compact spherical tokamak fusion pilot plant. *Philosophical Transactions of the Royal Society A: Mathematical, Physical and Engineering Sciences* 377(2141). doi: 10.1098/rsta.2017.0439.

Due to processes such as collisions between particles and turbulence, heat and particles are transported outwards across the separatrix. In the narrow region outside the confined volume towards the wall, the plasma particles and the heat get in contact with the wall. This happens in the thin, so-called "Scrape-off layer, SOL" between the confined plasma and the vessel wall (Stangeby, 2000) as shown in Fig. 2 adapted from Costley (2019). Particles which cross the separatrix onto the open magnetic field lines in the narrow, typically <1 cm, SOL can then be transported rapidly to the divertor. A smaller fraction diffuses further outwards and these particles are intercepted by the first wall.

Stationary and transient power loads

The plasma energy in the SOL despite effective magnetic confinement, is nevertheless high enough to cause severe damage to the materials facing the plasma. The most severe stationary power loads are expected to occur in the divertor of magnetic fusion devices at the so-called target plates shown in Fig. 2. There the highest heat loads of the order of 10–20 MW $\times$ m^{-2}, are expected in steady-state (Federici et al., 2001; Loarte et al., 2007; Pitts et al., 2011).

Moreover, instabilities in the plasma can lead to significant pulses of heat and particles being ejected into the SOL. In tokamaks, severe adverse effects may be caused by the so-called Edge-Localized Modes or ELMs (Hill, 1997; Stangeby, 2000) formed during the high confinement regime or H-mode (Wagner et al., 1982) and reviewed in greater detail in Zohm (2021) and in Jenko (2021). ELMs originate from plasma instabilities and eject the energy from the central confined plasma, shown in Fig. 2, towards the wall components (Stangeby, 2000). Edge-Localized Modes are capable of delivering several megajoules of energy within milliseconds to the wall components (Hill, 1997; Stangeby, 2000; Loarte, 2006) which can lead to localized melting and ablation of plasma facing surfaces at the divertor targets (Federici et al., 2017, 2018). Significant research activities have been implemented to establish means for either controlling the ELM frequency and amplitude, e.g. (Rapp et al., 2002; Baylor et al., 2012; Evans, 2013; Lang et al., 2013) or suppressing them completely, as described e.g. in (Evans, 2013; Loarte et al., 2015; Suttrop et al., 2018). ELM suppression is seen as a crucial aspect of designing plasma scenarios for a fusion reactor.

In addition to ELMs, tokamak disruptions can cause severe divertor thermal loads. Disruptions are global instabilities which can release the entire plasma stored energy on millisecond timescales, resulting in surface heat loads approaching 1 GW $\times$ m^{-2}. Extensive research is underway to predict, avoid, and mitigate disruptions in tokamaks (Hollmann et al., 2011; Lehnen et al., 2015).

Both the quasi-stationary power loads and transient power loads must be controlled carefully to ensure reliable operation of the plasma and to limit heating and erosion of the plasma facing surfaces thereby ensuring an acceptable lifetime for these surfaces.

The impinging plasma particles and intensive radiation from the plasma trigger complex plasma-material interactions (PMI) which will be described in detail later in the article. In the course of this explanation, we will review the particular impact of these processes on materials and describe the material concepts in use in present-day magnetic confinement fusion devices. Furthermore, we will describe solutions currently foreseen for the next generation of fusion devices and challenges to be addressed on the way to building a fusion power plant. We will review all material classes of magnetic fusion devices in this article. Due to the versatility of plasma-material interaction processes, their complexity and their crucial impact on the lifetime of fusion reactor, the plasma-facing materials will be discussed in greater detail.

Material challenge in magnetic confinement devices

Plasma-facing materials

Plasma—Material interaction processes

Plasma-material interaction (PMI) plays a crucial role in the choice of candidate materials suitable for the environment of fusion facilities. Among the most important are the following PMI processes:

- Sputtering of the wall materials by plasma particles
- Re-deposition of sputtered material, dust formation and transport
- Thermal loads to the plasma-facing components which can cause material melting
- Accumulation of radioactive tritium from the fusion plasma particles in the wall materials and its possible transport inside the materials of a fusion reactor
- Surface modifications and microstructure changes caused by the plasma particles and radiation

The main PMI processes see e.g. (Kirschner et al., 2016) are schematically shown in Fig. 3 (Kirschner, 2020) for the examples of beryllium (Be), molybdenum (Mo) and tungsten (W).

Physical sputtering

Electrons and ions in the core confined plasmas have energies of order of several keV. In the scrape-off layer plasmas, both electron and ion energies decrease significantly. Electrons, due to their low mass, cannot cause sputtering of material. In some cases the residual energy of plasma ions can exceed the threshold energy needed for sputtering of the wall material. The physical sputtering coefficient in the binary collision approximation depends on the masses of impinging and target particles as shown in the pre-factor for energy transfer:

$$\gamma = 4\, m_t m_p / \left(m_t + m_p\right)^2 \tag{2}$$

where m_t and m_p are the masses of the target material and the projectile respectively (Eckstein et al., 1993). Therefore, the most efficient sputtering occurs in the case of interaction of impinging and target particles of similar masses. Data on sputtering coefficients for most fusion materials can be found e.g. in Eckstein et al. (1993). The sputtering process leads to the reduction of the thickness of the plasma-facing material (PFM), which may adversely affect the lifetime of the entire component. The lifetime estimates for beryllium plates in the ITER fusion reactor (ITER Fusion Reactor Website, 2020), e.g. predict a surface recession of order of 0.01 mm for each plasma discharge due to sputtering (Borodin et al., 2011, 2019). Physical sputtering is frequently followed by processes of re-deposition of sputtered material and its subsequent re-erosion, leading to the stepwise process of so-called material migration in the fusion device.

The ejection of sputtered atoms into the edge plasma leads to core plasma contamination causing an adverse impact on plasma performance (Gruber et al., 2009; Mayer et al., 2009; Neu et al., 2009; Philipps et al., 2010; Tsitrone et al., 2011). Whereas sputtering increases with decreasing target mass, the plasma contamination impact increases super-linearly with increasing mass of the ejected atoms. Therefore, either low mass, i.e. minimized plasma impact or high mass i.e. minimized sputtering rate PFMs are preferred.

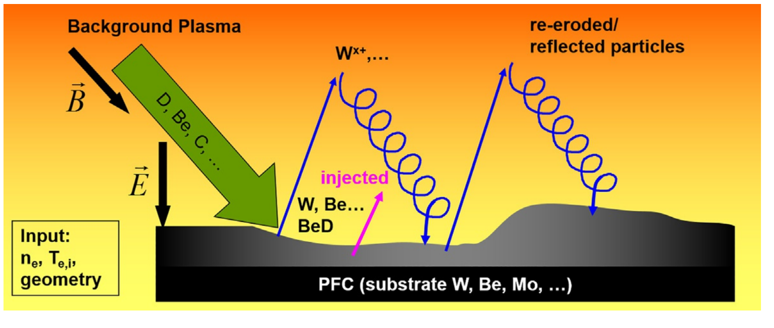

Fig. 3 Main processes of plasma-material interaction. Kirschner A (2020) PWI processes. Private communications.

Chemical erosion

The main plasma particles and the wall materials may possess a chemical affinity to each other and thereby undergo chemical reactions and build chemical compounds. The wall material will be then "consumed" in forming these compounds i.e. it will be eroded by chemically active particles. The corresponding process is called chemical erosion. The detailed description of chemical erosion can be found e.g. in Roth (2005). One of the most pronounced examples of plasma-facing materials prone to chemical erosion is carbon. Deuterium and tritium ions and atoms from the plasma interacting with carbon wall readily produce a variety of volatile hydrocarbons (Haasz et al., 1987; Pospieszczyk et al., 1999; Philipps et al., 2003; Roth et al., 2004; Jacob, 2005; Brooks et al., 2014). The hydrocarbons formed are then transported into the plasma and further to plasma-remote areas, such as e.g. pumping ducts. Chemical erosion processes are temperature-activated and their resultant erosion rate can even exceed that of physical sputtering. This happens e.g. in cases when the energies of impinging ions are still below the threshold for sputtering, whereas the temperature of the material and surrounding environment is already sufficient for chemical reactions to occur (Von Keudell and Jacob, 1996; Bohmeyer et al., 2005; Rudakov et al., 2007; Litnovsky et al., 2008; Wong et al., 2013).

Chemical reactivity is, strictly speaking, not necessarily an adverse effect in fusion plasmas. For instance, the chemical affinity of beryllium (Be) to oxygen—a common impurity in fusion plasmas—is effectively used in the JET tokamak to bind the oxygen to the beryllium walls thus forming an extremely stable and hard melting beryllium oxide, removing the oxygen from the plasma and thus purifying the edge plasma.

Fuel retention

Besides the material loss via chemical erosion, compounds formed may contain the plasma fuel particles: deuterium and tritium. Fuel accumulation represents a severe issue, since radioactive tritium e.g. in the form of volatile tritiated carbon compound, may travel long distances in the vacuum vessel until it finally reaches remote areas. Cleaning and conditioning of these remote areas are frequently challenging or even impossible. With time, such material transport and fuel co-deposition will lead to the undesirable accumulation of the radioactive fuel in the reactor (Dittmar et al., 2011; Litnovsky et al., 2011b; Koivuranta et al., 2013; Pégourié et al., 2013). Besides the radioactivity issue, transport of tritium to remote areas contributes to the loss of this costly element, which is indispensable for sustaining fusion reactions.

Some materials, like tungsten, have a low efficiency of tritium accumulation. Here, another issue may arise though. Once implanted into the material, tritium may start to diffuse deeper into the bulk and eventually penetrate into the coolant of the corresponding cooling systems. Increased chemical reactivity leading to a rapid degradation of the performance of cooling material in the tritium-containing environment is a known effect (Hayashi et al., 2006).

Fuel retention, accumulation and transport impose therefore, a significant concern. A set of measures is foreseen in order to minimize the tritium-driven effects. Certainly, a minimal affinity to tritium is desired from the plasma-facing materials and hence, low tritium retention. It is also known that increased temperatures lead to the prompt desorption of accumulated hydrogenic atoms (Roth et al., 2012; Atsumi et al., 1985; Brezinsek et al., 2013; Ryabtsev et al., 2016; Maier et al., 2019; Zlobinski et al., 2019). It will therefore be desirable to keep the operational temperature of the plasma-facing materials at the level of several hundreds of degrees centigrade. As an example, the first wall temperature of the future DEMO fusion power plant is expected to be in the range 600°C–730°C (Igitkhanov et al., 2013). Once tritium has penetrated into the bulk of plasma-facing materials, its transport can be stopped at the interface to the underlying structural material. For this purpose, so-called permeation barriers (Livshits et al., 1990; Levchuk et al., 2004, 2007; Pisarev et al., 2006; Nemanič, 2019; Houben et al., 2020) are being designed. The permeation barriers act, in a sense as a filter for tritium, preventing it from entering the structural material.

Recrystallization and melting

The heat loads on the PFMs can lead to temperatures significantly exceeding melting temperatures of corresponding materials. Plasma-facing materials in the divertor are at most risk. Melting in the divertor area has been extensively studied both experimentally (Coenen et al., 2011, 2015; Matthews et al., 2016; Krieger et al., 2018) and by modeling (Bazylev et al., 2011, 2014). However, accidental melting in the main chamber has also been reported (Matthews et al., 2016). A photograph of a re-solidified melted fragment from the inner wall limiter in JET is presented in Fig. 4. In tokamaks, severe adverse effects may be caused by the ELMs and disruptions described above.

Melt damage is dangerous in itself. After melting, the damaged area often solidifies in a shape which protrudes towards the plasma and intensifies melting and splashing of molten material during the subsequent plasma operation. Such behavior was observed in melting experiments reported both in divertor (Coenen et al., 2015, 2017; Matthews et al., 2016; Krieger et al., 2018) and limiter tokamaks (Sergienko et al., 2007; Bazylev et al., 2011; Coenen et al., 2011). The molten layer experiences current flowing through it. Being located in a magnetic field, the motion of the molten layer is dominated by the $J \times B$ force which, depending on geometry, may even exceed the gravity force (Sergienko et al., 2007; Coenen et al., 2011; Matthews et al., 2016). The molten layer of e.g. heavy tungsten may exhibit an unusual property of moving upwards, depending on location of the molten surface.

Resistance to thermal loads and the corresponding avoidance of surface damage and melting is not solely a function of specific material choice, but also of material geometry. Shaping of plasma-facing components becomes necessary for fusion devices. Here, experience from dedicated studies in MCF devices (Litnovsky et al., 2005b, 2011b; Tanabe et al., 2005; Wong et al., 2007; Krieger et al., 2007; Litnovsky et al. 2007a,b, 2009; Rudakov et al., 2009b; Ding et al., 2014; Hong et al., 2014) coupled with modeling (Dejarnac and Gunn, 2007; Komm et al., 2011; Matveev et al., 2014), can be harnessed for construction of the advanced shapes

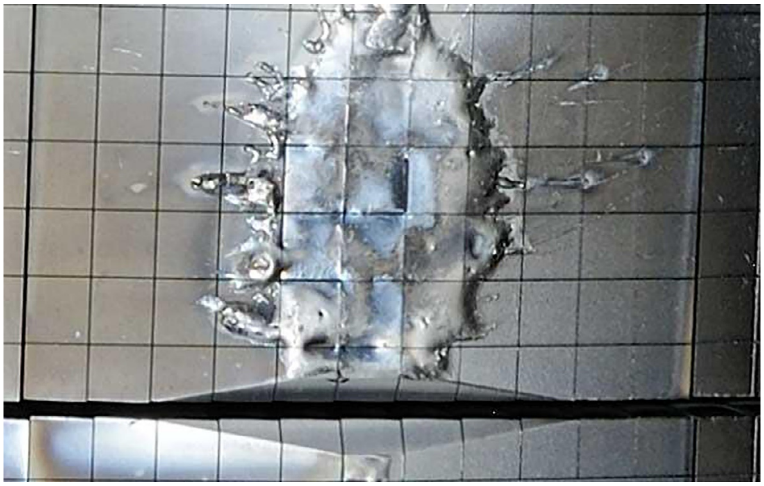

Fig. 4 A photograph of a re-solidified area of a beryllium plasma-facing component in the JET tokamak following a melting event. Matthews GF, et al. (2016) Melt damage to the JET ITER-like wall and divertor. *Physica Scripta* T167: 14070. doi: 10.1088/0031-8949/t167/1/014070.

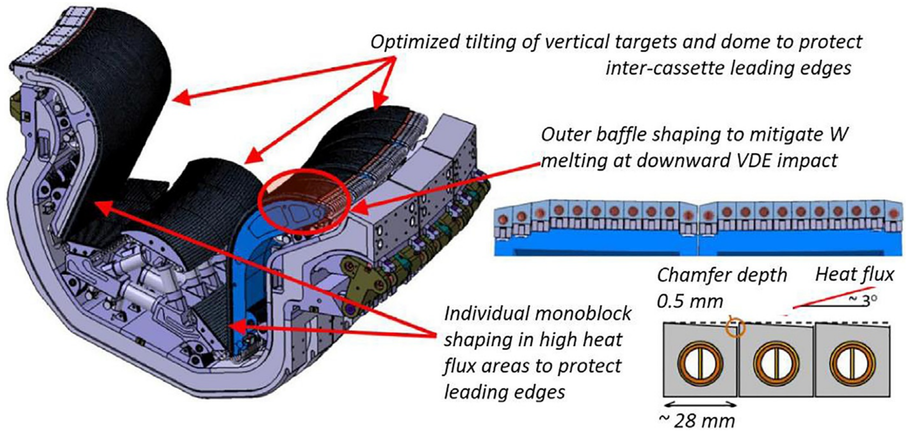

Fig. 5 Shaped plasma-facing components of the tungsten divertor of ITER. Hirai T, et al. (2016) Use of tungsten material for the ITER divertor. *Nuclear Materials and Energy* 9: 616–622. doi: 10.1016/j.nme.2016.07.003.

required for future plasma-facing components (Litnovsky et al., 2007b; Pitts et al., 2011, 2019; Stangeby, 2011; Hirai et al., 2016). An example of shaping of the tungsten plasma-facing components in the ITER divertor is provided in Fig. 5.

Dust formation and transport

Co-deposition of sputtered material with the fusion fuel, sometimes followed by prompt re-erosion of freshly deposited layers, their further re-deposition and hence, the further transport of the material frequently leads to the formation of thick deposits. Adhesion of those deposits to the surface is usually rather poor, which leads to their flaking. Flakes or larger fragments of material are usually called dust. The dimensions of dust particles varies greatly, from several tens of nanometers to several millimeters. Hence the effects caused by dust are rather diverse: dust may be fairly harmless, disappearing in the remote areas of the machine and sometimes, not even being noticed and, in the other extreme, dust can cause severe plasma contamination, finally leading to radiative collapse and to a plasma disruption and quench (Winter, 1998, 2004; Krasheninnikov et al., 2005, 2008; Rudakov et al., 2009a; Rubel et al., 2018).

The effects of dust were extensively investigated using various diagnostic techniques (Smirnov et al., 2009; Bergsåker et al., 2011; Kantor et al., 2013; Litnovsky et al., 2013; Shalpegin et al., 2015; Tolias et al., 2016). Dedicated studies show that the fraction of dust mobilized from wall surfaces into the plasma is rather small and not exceeding 20% of the entire amount of dust (Litnovsky et al., 2013). Most dust particles travel to the pump ducts or become stuck in hidden areas and gaps of the first wall and divertor. At the same time, dust mobilized into the edge plasma may travel distances as large as several meters in the plasma volume before they are ablated (Krasheninnikov et al., 2005, 2008; Smirnov et al., 2007; Litnovsky et al., 2013; Lazzaro et al., 2020). Dust entering the core plasma volume is rather rare and its effect usually vanishes after several milliseconds of plasma discharge (Rudakov et al., 2009a; Litnovsky et al., 2013). If dust does enter the core plasma, its ablation will provide a massive source of impurities which causes unacceptable radiative losses and eventually, leads to plasma collapse due to the loss of density control. The amount of allowed impurities in the core plasma is negligible. For instance the allowable amount of tungsten estimated for a core plasma of ITER is limited to some 0.001% of the main fuel particles (Pütterich et al., 2010). The detected re-mobilization of dust particles increases the residence time of dust in plasmas and degrades the plasma performance further (Ratynskaia et al., 2013; Tolias et al., 2016).

Besides the issues of radiation and plasma control impact, dust may impose a radioactivity hazard by the accumulation and transport of tritium to remote areas. Furthermore, because of its small size, great particle number and hence, large total reaction area, under some conditions dust may pose an explosion hazard, as reviewed in e.g. Grisolia et al. (2009) and may introduce safety hazards during off-normal events that mobilize the in-vessel inventories (Sharpe et al., 2002, 2005; Petti et al., 2006; Skinner et al., 2008). Dust handling represents a cornerstone element in licensing of future fusion facilities (Van Dorsselaere et al., 2012; Perrault, 2016; Wu et al., 2016).

Surface and structure modifications, blistering and fuzz formation

Interaction with plasma particles leads to a series of changes both in microstructure and on the surface of plasma-facing materials (Ueda et al., 2014). Corresponding investigations are underway both in the MCF devices (Bernard et al., 2015; Tokitani et al., 2017) and laboratory facilities (Baldwin and Doerner, 2008). Dedicated modeling (Krasheninnikov, 2011; Martynenko and Nagel', 2012; Trufanov et al. 2015) is used to address these changes and to reveal the underlying physics mechanisms.

Plasma-material interaction may lead to e.g. formation of bubbles and blisters (Shu et al., 2007a,b; Miyamoto et al., 2009; Kajita et al., 2011; Yamagiwa et al., 2011; Juslin and Wirth, 2013; Ueda et al., 2014), needle-like structures, sometimes called whiskers (Chih et al., 2011; Doerner et al., 2014; Kreter et al., 2014) and the more complicated structures, called fuzz, see e.g. Ueda et al. (2014). The formation of blisters and fuzz are among the most widespread effects and presently attract the most attention. Blisters are cavities created by implanted and diffused plasma particles: H, D, T and He accumulated beneath the surface of metals. Blisters are therefore filled with a gas. The size of blisters varies depending on environmental conditions, ranging from several nanometers up to several hundreds of micrometers. Depending on conditions, blisters can either grow or break leading to the gas release and, more importantly, trigger crack formation (Hong et al., 2014). Numerous studies (Shu et al. 2007a,b; Miyamoto et al., 2009; Hong et al., 2014; Ueda et al., 2014) were conducted showing that blister evolution is very sensitive to the elemental composition of impinging particles (Shu et al., 2007b; Ueda et al., 2014), their energy (Buzi et al., 2014), structure of plasma-facing material (Manhard et al., 2017), the temperature of the material (Ueda et al., 2014) and its crystal orientation (Shu et al., 2007a). A concise physics understanding and evaluation of blister formation are still to be attained.

Fuzz formation is another effect triggered by plasma-material interaction. Under specific conditions of high flux and correspondingly, high fluence of helium ions, and at surface temperatures in the range of several hundred degrees centigrade, the formation of the thin, nanometer-sized and long (hundreds of nanometer in length) column-like structures—"fuzz" is routinely observed (Baldwin and Doerner, 2008; Kajita et al., 2009; Gasparyan et al., 2016). Fuzz is usually formed on the surface of heavy metal plasma-facing materials, like tungsten. Unlike blisters with clearly detrimental effect on consistency and mechanical properties of the exposed material, there is no consistent opinion on the role of the fuzz in plasma-material interaction. On one hand, the surfaces with fuzz are expected to be vulnerable to heat loads (Ueda et al., 2011;Brezinsek et al., 2017b). On the other hand, modeling studies e.g. Krasheninnikov (2011) predict the fuzz in fact, to be more stable than the solid substrate material to the sputtering due to relatively small partial area of the fuzz, which can be hit by plasma particles and become sputtered without a prompt re-deposition to the neighboring fuzz structure. As in the case for blisters, the formation of fuzz is highly dependent on environmental conditions in a fusion device. Presently, it is assumed that the growth of fuzz is dependent on competing erosion of fuzz structure and its annealing due to transient heat loads (De Temmerman et al., 2019). The formation of deposits covering fuzz was detected on the tungsten surface of a material test-sample in the divertor of ASDEX Upgrade (Brezinsek et al., 2017b), whereas the pre-grown fuzz placed in the outer SOL plasmas of TEXTOR vanished within a few plasma discharges (Ueda et al., 2011).

Plasma-facing materials: Material choice

The processes of plasma-material interactions discussed above represent a severe challenge for candidate materials needed for the next generation of MCF devices like ITER and further, for a fusion power plant. The optimum plasma facing material should simultaneously possess several, in part contradictory, properties in order to be compatible with the harsh fusion environment. The most important, almost compulsory, properties include:

- Low tritium retention
- Low sputtering yield by plasma particles
- High thermal conductivity at elevated temperatures above 200°C
- As low as possible neutron-induced radioactivity in fusion environment
- Wherever possible, low chemical activity
- Wherever possible, ability to capture or bind plasma impurities

Here we briefly review past, current and prospective candidate materials and concepts.

Carbon and carbon composites

For several decades, carbon (Merola et al., 2004) was one of the most widespread PFMs for fusion devices (Barabash et al., 1999; Duffy, 2009). Its extraordinary properties, such as absence of melting, very high thermal conductivity, even further enhanced in the so-called carbon fiber composites (Snead and Ferraris, 2020), low brittleness and hence, easy machinability are some of the most attractive features of carbon. However, carbon is prone to chemical erosion of carbon (Mech et al., 1998; Philipps et al., 2003; Roth, 2005) described above. Volatile hydrocarbons can travel long distances. Since radioactive tritium reacts with carbon, the so-called long range transport (Wienhold et al., 1999, 2003; Matthews, 2005) can lead to tritium accumulation in poorly accessible areas of the fusion reactor. Being a light element, carbon is prone to physical sputtering by plasma particles (Eckstein et al., 1993). These properties and their implications for reactor operation, have ultimately disqualified carbon as a prospective fusion material (Neu et al., 2009; Pitts et al., 2011; Hong et al., 2015).

Beryllium

Beryllium (Be) has received significant interest as a plasma-facing material within the fusion community, in particular in existing fusion experiments such as JET. Beryllium, still being a light element with rather high physical sputtering vulnerability (Eckstein et al., 1993), features greatly suppressed chemical erosion when compared with that of carbon (De Temmerman et al., 2008; Carpentier et al., 2011). At the same time, beryllium possesses an excellent capability to binding oxygen (Winter, 1996; Tomastik et al., 2005; Konings et al., 2012; Wauters et al., 2020)—a highly deleterious impurity for fusion plasma performance responsible for undesirable radiative cooling of the plasma (Breton et al., 1976; Rogerson et al., 1977; Morozov et al., 2007) and for the enhanced sputtering of plasma-facing materials. Beryllium is therefore, the candidate material for the first wall of fusion devices where particle, thermal and neutron loads are rather benign.

The application of beryllium in a fusion power plant would be however, impossible. As a light material, Be would be subject to intolerable sputtering and material losses during a quasi-stationary operation. A fusion power plant will feature extremely high neutron fluence as compared to that of any present MCF device including ITER. In the course of neutron irradiation, Be will be a subject to transmutation leading to the formation of primarily ^{10}Be, ^{7}Li, and ^{6}Li (M R Gilbert and Sublet, 2016), as well as significant gas formation, particularly from helium ^{4}He, ^{3}He which could cause embrittlement problems (Martin and Ellis, 1963; Gelles et al., 1994; Kesternich and Ullmaier, 2003; Gilbert et al., 2012).

Tungsten

Achievements in plasma position control (Cenedese and Sartori, 2004; De Tommasi, 2019), well-developed scenarios for auxiliary heating (Gruber et al., 2009) have returned heavy metal options as future plasma-facing materials (Mayer et al., 2009; Neu et al., 2009; Brezinsek et al., 2017a; Pitts et al., 2019) into consideration. Tungsten (W) with its excellent thermal conductivity, low sputtering yield with respect to light plasma particles, highest melting temperature among non-ceramic materials, low tritium retention and moderate activation by fusion neutrons is deemed presently to be the best choice for plasma-loaded areas, like the divertor (Loarte et al., 2007; Pitts et al., 2011).

A material mix: Be for the first wall and W in the divertor, has been successfully used for plasma-facing materials in JET (Matthews et al., 2007; Philipps et al., 2010). In recent years, tungsten was successfully applied as a PFM in large MCF devices: besides JET, tungsten is used in ASDEX Upgrade (Neu et al., 2009) for the entire coverage of the first wall and divertor as well as in WEST (Missirlian et al., 2014; Firdaouss et al., 2017). There are also plans to make a tungsten divertor in JT 60SA. After the successful attempt with tungsten in LHD (Tokitani et al., 2019), this material is currently under the consideration for the future divertor in the Wendelstein 7-X advanced stellarator in Germany.

There are also disadvantageous properties of tungsten. Fusion plasma is highly sensitive to tungsten as an impurity (Pütterich et al., 2010), since this material radiates very effectively leading to undesirable radiative loss of fusion energy in the core plasma. Melting of tungsten may impose the issue, especially during transient events (Coenen et al., 2011; Matthews et al., 2016; Krieger et al., 2018) or re-attachment of the divertor plasma (Bonnin et al., 2017; Eldon et al., 2017). Recrystallization of tungsten in the course of thermal excursions (Guo et al., 2018; Morgan et al., 2020) may change its mechanical properties and affect the exploitation of the plasma-facing components. Tungsten exhibits an extensive crack network developed under repetitive heat loads (Klimov et al., 2011; Herrmann et al., 2017; Zammuto et al., 2018), which may lead to thermal fatigue failure. Tungsten oxidizes readily at elevated temperatures and the oxide of tungsten is volatile. At room temperature, pure tungsten is a very brittle material and its machining is a challenging task. Under these circumstances, the use of pure tungsten in a future fusion power plant is deemed to be problematic. New, advanced materials are being created, significantly expanding the functionality of pure tungsten as needed for the power plant application.

Advanced plasma facing materials

We have reviewed the current challenges in selecting a suitable plasma-facing material for the construction of near-future fusion experiments. For the next ultimate step—the fusion power plant, PFM challenges will increase significantly. Whereas the plasma parameters are not expected to differ greatly from those expected in the ITER experiment, the key difference is much higher particle and especially, neutron fluence. The severe neutron environment will bring new effects adversely affecting material performance. Another significant challenge will be to maintain the thermo-mechanical functionality of plasma-facing materials throughout the entire service life of the power plant. This may lead, possibly, to an avoidance of specific plasma scenarios. A third significant challenge is due to significantly increased safety requirements imposed on a quasi-stationary power plant. The costs and availability of the source materials and technological feasibility of the component manufacturing are important factors, too. The analyses of new aspects influencing the fusion materials (Maisonnier, 2005; Coenen et al., 2016; Federici et al., 2017; Wenninger et al., 2017; Coenen, 2020) have outlined the necessity of the advanced material concepts. Advanced materials possess unique features, significantly extending the properties of conventional materials in critical areas of their functionality. The development of advanced materials has been focused on four main directions:

- Doped tungsten
- Tungsten composites
- Binary solid solution alloys
- Multi-component alloys

An extensive summary of the mentioned concepts is provided in e.g. Rieth et al. (2019). Usually, advanced material is being developed using a combination of element selection and advanced technology thus representing the material concept. We will briefly review a few mostly advanced material concepts.

Intrinsic properties of tungsten, such as its brittleness at room and elevated temperature were improved using cold rolling combined with thin plate preparation technology, applied successfully for the production of tungsten laminates (Reiser et al., 2017). The remarkable feature of these laminates is their engineered ductility even at room temperature.

Tungsten fiber composites or W_f/W, have been introduced in order to extend the applicability and robustness of tungsten, especially during cyclic high heat loads (Riesch et al., 2014; Jasper et al., 2016; Coenen et al., 2018). Millimeter-size tungsten fibers with a diameter of about 150 microns are introduced into a tungsten matrix (Jasper et al., 2015; Coenen et al., 2018; Mao et al., 2018, 2019a,b, 2020). Fibers are coated with an interface layer of erbia Er_2O_3 or yttria Y_2O_3 having a typical thickness of several microns, ensuring a weak interface between the fiber and the matrix. The main idea behind the tungsten fiber materials is in the dissipation of energy, which otherwise would feed into the buildup of stresses, crack propagation and finally, to the destruction of the component. The W_f/W features an unique pseudo-ductility and therefore, is much more resilient against damage than monolithic tungsten (Coenen et al., 2018; Mao et al., 2020). Another promising concept is the so-called microstructured W, where an array of millimeter-size tungsten tubes with diameter of $\sim$150 μm is directly integrated into the heat sink material. Microstructured W has already demonstrated impressive results by surviving extreme repetitive high heat loads expected in the divertor area (Terra et al., 2019) without a damage.

Significant progress was attained in production of tungsten components using the so-called power-injection molding (PIM). In this process, the tungsten powder is fed into a cavity where it is pressed into the desired form using high pressure. The significant advantages of PIM is the speed of the process and the ability to obtain components of practically any shape and geometry (Antusch et al., 2011).

Another promising concept, self-passivating (Koch and Bolt, 2007; Koch et al., 2009, 2011), so-called "smart" tungsten-based alloys (López-Ruiz et al., 2011; García-Rosales et al., 2014; Litnovsky et al., 2017a,c,d) has been proposed for the first wall of the future fusion power plant. During regular operation, smart alloys should exhibit advantages of a pure tungsten plasma-facing surface. During an accident, the alloying elements in the bulk form a protective layer and prevent the sublimation of neutron-activated tungsten oxide into the atmosphere. Modern tungsten-chromium yttrium smart alloys feature at least 10^4-fold suppression of oxidation (Wegener et al., 2016, 2017; Litnovsky 2017c; Klein et al., 2018a) and more than a 40-fold reduction of sublimation (Klein et al., 2018b). Photographs of smart alloys and pure tungsten before and after exposure under accident conditions are shown in Fig. 6. Plasma tests (Litnovsky et al., 2017d; Schmitz et al., 2018, 2019) confirmed a similar sputtering resistance of smart alloys and tungsten to deuterium plasma under conditions expected at the first wall of a fusion power plant (Litnovsky et al., 2020; Schmitz, 2020).

New alloys with a controlled microstructure were developed for application in a high neutron flux environment feature reduced recrystallization and high tensile strength under extreme conditions (Kurishita et al., 2010; Nogami et al., 2020). This promising concept of so-called nano-engineered alloys was pursued in (Zhang et al., 2017). The small nanometer-size chromium inclusions are formed between the tungsten grains in tungsten-chromium and tungsten-chromium-titanium alloys. The formation of nano-size chromium-rich phase effectively opposes recrystallization and grain coarsening under neutron irradiation and temperature excursions.

Studying the effects caused by neutron irradiation are a vital part of the testing and qualification of materials for a future fusion power plant. In particular, the damage produced by neutrons and corresponding transmutation is a focus of these investigations. Several approaches exist to study in particular, the neutron damage, such as e.g. ion self-damage see e.g. Markelj et al. (2013) and exposure to fission neutrons. However, comprehensive testing under fusion relevant conditions is only possible with a fusion-relevant neutron source (Gilbert and Sublet, 2017). The International Fusion Materials Irradiation Facility—DEMO Oriented Neutron Source (IFMIF-DONES) is the major facility presently under construction to address the effects caused by fusion neutrons on materials (IFMIF DONES Facility, 2020). The IFMIF-DONES facility is reviewed in Donne et al. (2021).

Liquid metals

Liquid metals represent another, unique class of plasma-facing materials under investigation. Unlike the solid metals described above, where extreme care was taken to preserve the initial surface and microstructure, in the concept of the liquid first wall these

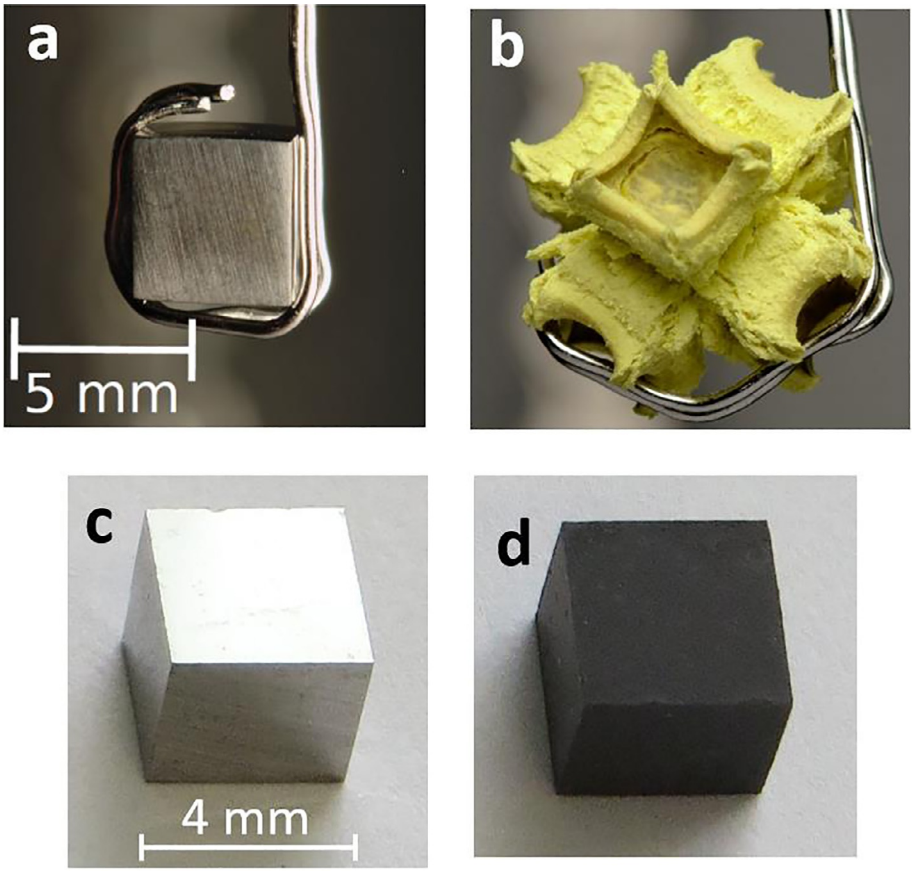

Fig. 6 Photographs of a pure tungsten sample and a tungsten-based smart alloy exposed under accident conditions as expected in DEMO power plant: (A) tungsten sample before exposure; (B) oxidized tungsten sample after exposure; (C) smart alloy sample before exposure and (D) smart alloy sample after exposure.

properties are discarded from the beginning. Instead, a constant renewal of the liquid metal surface is the fundamental feature of liquid metal application (Nygren and Tabarés, 2016; Ruzic et al., 2017; Zakharov, 2019), thus mitigating the issues mentioned, such as erosion and surface and transient damage. Many approaches to realize the liquid metal first wall have been investigated, ranging from a free molten surface (Ono et al., 2017; Yang et al., 2017) to a rather sophisticated, but the most promising, self-sustaining surface realized via a capillary porous structure, CPS (Evtikhin et al., 2002b; Khripunov et al., 2003; Mirnov et al., 2006; Lyublinsky et al., 2007; Coenen et al., 2014). In the CPS, the stability and the adherence of the metal molten layer is maintained by the capillary forces acting on the metal melt that soaks through the supporting metal mesh of submillimeter size. Several candidate materials are presently under investigations (Mazzitelli et al., 2011), such as lithium (Lyublinsky et al., 2007) and tin (Lyublinski et al., 2016; Roccella et al., 2020). Lithium is among the most promising materials, due to its low melting temperature, low Z number and the possibility of using it as tritium breeder in the fusion power plant (Evtikhin et al., 2002a; Nagayama, 2009). Laboratory studies have demonstrated the superior ability of a lithium liquid surface to withstand the high heat loads exceeding 20 MW/m^2 (Khripunov et al., 2001) by evaporating and creating a dense and cold lithium plasma in front of the liquid metal surface (Khripunov et al., 2001). It was shown that most of the power dissipation is realized through the vaporization of lithium. Successful realization of prototype first wall components have been reported from present day devices (Mirnov et al., 2006; Mazzitelli et al., 2011; Ono et al., 2017), where liquid metal structures, mostly CPS, were installed both in the divertor area (Ono et al., 2017) and as a part of the first wall. Among the challenges imposed by realization of the liquid metal solution are the recycling of lithium and re-liquidation of the molten layers and the collection and re-feeding of lithium to the first wall structures. An important issue is the transport of the vapor created by plasma-material interaction and the re-solidification of lithium in remote, usually cold and hardly accessible parts of the MCF device, causing metal contamination of the sensitive, mostly optical, diagnostic components (Khripunov et al., 2001). Uptake of deuterium and tritium via lithium layers, prompt creation of lithium hydrides and their subsequent transport to the distant areas and, potentially, into the inner structures of the device represent a critical issue for the application of liquid metals as PFMs for a fusion power plant (Ono et al., 2017). Intensive R&D efforts are currently underway to address the mentioned issues and several proposals for the first wall and divertor components of the power plant have been created and are proceeding towards realization (Evtikhin et al., 2002a; Nagayama, 2009; Morgan et al., 2018).

Blanket materials

In a fusion power plant, the plasma-facing first wall and the breeding blanket will constitute a common structure. The purpose of the blanket is the breeding of tritium needed for the tritium self-sufficiency of the fusion power plant as reviewed in detail by L.V. Boccaccini in (Boccaccini, 2021). The blanket must, in addition, play a major role in transferring the heat to the heat exchangers and finally, in converting the heat to electricity. The blanket structure is, therefore, crucial for the success of the controlled nuclear fusion concept (Stork et al., 2014a,b; Stieglitz et al., 2018; Federici et al., 2019). Depending on the blanket construction, a dedicated neutron multiplier may be used. Alternatively, the breeding material of the blanket itself will be used as a neutron multiplier. Presently, there are several blanket concepts under the development. These concepts can be divided into three main types:

- liquid metal concepts;
- ceramic breeder concepts;
  and recently proposed
- concepts based on molten salt, is considered in the end of this section

In the liquid metal concepts, either pure lithium or lead-lithium eutectic alloy (PbLi) is used. There are two essentially different design solutions for the liquid metal blankets. In the single-coolant design, the liquid metal will be used both for breeding and for cooling of the blanket structure, whereas in the dual-coolant concept, liquid metal is used for breeding only and a separate coolant, water or helium, is used for cooling.

Among the most developed liquid metal breeder concepts are:

- Water-cooled lead-lithium blanket (WCLL)
- Helium-cooled lead-lithium blanket (HCLL)
  and
- Dual-cooled lead-lithium blanket (DCLL)

In the solid breeding blanket concepts, a solid medium in the form of ceramic pebbles or spheres is enclosed in the body of the beryllium neutron multiplier. Among the known and most developed concepts are:

- Helium-cooled ceramic blanket (HCPB)
- Helium-cooled ceramic breeder graphite collector (HCCR)
- Water-cooled ceramic breeder (WCCB)

Blanket construction is rather complex, comprising the cooling, tritium extraction, coolant purification and instrumentation systems and control subsystems. The principal blanket concepts are presented and assessed in e.g. Giancarli et al. (2012), and Abdou et al. (2015). It is planned to test the major breeding blanket concepts: HCLL, WCCB and HCCB, in ITER environment using the so-called test blanket modules (Boccaccini et al., 2004; Giancarli et al., 2012; Boccaccini, 2013; Abdou et al., 2015; Zmitko et al., 2017). In ITER, however, the tritium breeding efficiency and effective heat production cannot be tested due to insufficient neutron fluxes (Giancarli et al., 2012; Abdou et al., 2015) at the ITER first wall. Nevertheless, the entire construction of the blanket can be evaluated, including the consistent functioning of all essential subsystems and the results can be used for further extrapolative modeling (Giancarli et al., 2012). There are several proposals for the future full functional test of the breeder solutions, including the building of a dedicated Fusion Science Nuclear Facility, as proposed by the United States.

Operation of the breeding blanket is accompanied with several, in part crucial, issues and risks. Among those, the interaction of a slowly moving conductive liquid metal with a strong magnetic field, which causes significant Lorentz forces. In several concepts, such as DCLL and HCLL, insulating so-called flow channel inserts (FCIs) are foreseen in order to minimize these conductive circuits and hence, to limit the electromagnetic forces acting on the blanket. The structure of the blanket is expected to be made from magnetic steel. The use of magnetic material leads to stresses in the construction and may distort the magnetic field configuration in the power plant, especially during the ramp-up and ramp-down phases of plasma operation (Zmitko et al., 2017). Finally, general safety and tritium isolation impose severe requirements on tritium permeation, efficient evacuation and containment. In general, the following requirements are specified for blanket materials:

- Neutron robustness, reduced activation
- Tritium opacity
- Reduction of electromagnetic forces
- Thermo-mechanical stability of the entire construction

Generally, the principle of Reliability/Availability/Maintainability/Inspectability (RAMI) (Abdou et al., 2015) is applied to the entire blanket construction. The application of RAMI to materials used in blanket construction has led to the material selection described below. There are three classes of functional blanket materials: the structural materials, the materials for flow channel inserts and the tritium permeation barrier (TPBs) materials.

For the structural blanket materials, reduced activation ferritic-martensitic steels (RAFMs) are selected. In the European HCLL and HCPB concepts, the use of Eurofer (Van der Schaaf et al., 2003; Möslang et al., 2005; Boccaccini, 2013; Tassone et al., 2018) is foreseen, whereas in the WCCB concept proposed by Japan, the F82H RAFM steel is planned as a structural material (Giancarli et al., 2012; Tanigawa et al., 2017). Significant R&D activity is underway in order to assess, among others, the interaction of helium coolant with RAFM as well as the complex interaction with the PbLi (Flament et al., 1992; Tortorelli, 1992; Malang and Mattas, 1995; Moreau et al., 2011; Abdou et al., 2015; Zmitko et al., 2017).

For flowing channel insulation the main candidate solution is silicon carbide (SiC). The use of SiC for FCIs, in bulk or in dense foam form brings several advantages, such as significant reduction of the MHD loads and a rise of operation temperature to about 700°C. Such a high operation temperature however, exceeds the current temperature window of the RAFM application (Möslang et al., 2005; Abdou et al., 2015; Tanigawa et al., 2017; Tassone et al., 2018). In addition, the high temperature response of SiC to neutron irradiation, as well as technological concerns of manufacturing the complex geometries of FCIs out of SiC, need further exploration. The potential interaction of FCIs with the e.g. PbLi eutectic and RAFM are among potential concerns (Pint et al., 2007; Muroga, 2012; Abdou et al., 2015; Smolentsev et al., 2015). The use of alumina (Al_2O_3) as an alternative to SiC is still under assessment. Here, the radiation hardness and activation properties are among major concerns (Abdou et al., 2015).

Tritium permeation barriers have to be implemented within the blanket structure. Their role in the breeding blanket becomes even more important, since the TPBs must warrant efficient containment, and refill the bred tritium to the power plant, including the reservoir systems to be used in case of blanket failure (Abdou et al., 2015). Permeation barriers under development (Livshits et al., 1990; Levchuk et al., 2004, 2007; Pisarev et al., 2006; Houben et al., 2020) are already providing an efficient tritium isolation. Modern barriers made of yttria (Houben et al., 2020) may provide more than a 10^6-fold decrease of tritium flux permeation to the bulk of the facility in the temperature range of 300°C–600°C (Houben et al., 2020).

In the blanket environment, the reactions with liquid breeder and coolant, as well as possible interactions with structural materials and FCIs, must be investigated. Performance studies of neutron-irradiated TPBs are of crucial importance for the breeder blanket.

As mentioned above, the interaction of the working fluid or solid breeder and neutron-multiplier materials with the functional elements of the blanket, is important. The chemical and mechanical durability of breeder and multiplier materials themselves represents a crucial topic for the blanket feasibility. We will not provide a comprehensive overview of all issues and open questions in the section, but mention a few. The use of beryllium as neutron multiplier in e.g. ceramic breeders faces issues due to the radiation-induced volumetric swelling, reaching 16% at 650°C (Abdou et al., 2015; Fedorov et al., 2016). The use of the beryllium intermetallic phase $Be_{12}Ti$ seems advantageous in this respect. However, water-beryllium interaction in the case of liquid blankets imposes problems (Abdou et al., 2015). For the dual-coolant systems, such as DCLL, the permeation of bred tritium into the helium-coolant circuit is considered as critical, imposing stringent requirements for TPBs.

In relation to the molten salt concepts noted above, the main potential advantage of using e.g. F-Li-Be or F-Li-Na-Be salts is their low electrical conductivity. This would alleviate the MHD issues of the conductive medium. Molten salts are also relatively chemically inert. At the same time, their high viscosity and high melting point limit the operating window severely. In addition, under neutron irradiation, the corrosive interaction of molten salts with the interior of the blanket, leading to the potential release of highly active and toxic fluorine, represents a significant concern.

Diagnostic materials

Another class of materials in MCF devices which are at least partly exposed to plasma particles are the materials of diagnostic components. Here, the difference between the present-day devices and the coming experiments, e.g. ITER, is rather distinct. The particle, neutron and radiation environment in present-day devices is rather benign and the plasma pulses are usually limited to several seconds. A wide range of materials can be used without any significant risk or degradation of performance or with relatively easy exchange possibilities. On the contrary, in the devices of ITER-class, the neutron and radiation fluxes are orders of magnitude larger (Costley et al., 2001, 2005; Walker et al., 2005; Donné et al., 2007) than those in any of the present MCF devices, and hence cannot be neglected. In the following description, we will focus on diagnostic material challenge for fusion devices of the ITER-class and for the fusion power plant.

Due to the harsh neutron environment, the use of refractive optical elements i.e. lenses and prisms, will be impossible in these MCF devices, mostly due to the inability of the corresponding materials to withstand neutron irradiation (Voitsenya et al., 2001; Voitsenya and Litnovsky, 2009). A reflective, mirror-based option will be used instead. Diagnostic mirrors will guide the plasma radiation towards spectrometers and detectors (Costley et al., 2001; Donné et al., 2007; Litnovsky et al., 2019a). The first optical element directly viewing the plasma is the so-called first mirror. It is one of the most important diagnostic elements overall, given the number and importance of optical diagnostics and the fact that the performance of the entire corresponding diagnostic largely relies on the performance of its first mirror and hence, on the mirror material. Moreover, it will become necessary to clean the mirrors from the deposited material eroded from the first wall and the divertor—these processes are described earlier in the sub-chapter "Plasma-material interaction processes". The repetitive cleaning will be performed in situ using a local plasma for sputtering the impurities from the mirror surface (Litnovsky et al., 2011a, 2015, 2019b; Mukhin et al., 2012; Moser et al., 2015; Leipold et al., 2016; Peng et al., 2018; Yan et al., 2018). Single crystal mirrors made from highly reflective materials, such as molybdenum and rhodium are among the main candidates for the diagnostic mirrors (Voitsenya et al., 2001; Litnovsky et al., 2005a, 2007c, 2017b, 2019b; Matveeva et al., 2010; Peng et al., 2018). Mirrors coated with a reflective molybdenum or rhodium layer are under investigation (Marot et al., 2007; Eren et al., 2011). As for the further, more distant, secondary mirrors, the environmental conditions are not as restrictive and therefore the choice of materials increases. Currently, stainless steel and aluminum mirrors coated with protective sapphire or tantalum oxide Ta_2O_5 layers are being considered (Mukhin et al., 2008a). Alternatively, secondary mirrors with titanium dioxide and silica highly reflective layered coating oxide are under study (Krimmer et al., 2013); however, attaining the desired long-term performance is challenging.

For some diagnostics (Mukhin et al., 2008b, 2009), protective windows are foreseen. Windows will be used as well as vacuum isolation for several diagnostics. Fused silica, sapphire and quartz are presently the main candidate window materials (Aymar, 2002). As for duct and corresponding support structures, most diagnostics are expected to use steel (Kalinin et al., 2000; Voitsenya et al., 2001; Krasikov et al., 2011). For fusion power plants, the choice will most probably be made in favor of reduced-activation steels due to the increased neutron irradiation. These steels are described in detail in the next section.

Material choice for the other elements of the reflective optical paths, such as fiber bundles, appears to be challenging. A range of neutron-induced changes or effects, such as radiation-induced electromotive effect, radiation-induced conductivity, radiation-induced electric degradation and generally, non-ohmic behavior, may affect the performance and degrade the lifetime of the fiber materials (Zinkle, 1994; Aymar, 2002). Current studies show advantages from using mineral insulated cables (Vayakis et al., 2008). However, care must still be taken to avoid radiation-induced effects (Vila and Hodgson, 2009), depending on their chemical and elemental purity of the fiber material (Hodgson, 1998). Similar issues with radiation-induced effects will be experienced by the other diagnostic components such as e.g. imaging bolometers (Peterson et al., 2008).

In a fusion power plant, the requirements for diagnostic materials and assemblies will likely be even more demanding. Only a few crucial optical diagnostics will remain, and mirrors should be of reduced size and placed far away from the plasma (Orsitto et al., 2016; Biel et al., 2019). In addition, reserve optical channels should be foreseen to ensure continued operation in case of the failure of the main diagnostic (Litnovsky et al., 2010; Biel et al., 2019).

Structural materials

The main function of structural materials in current plasma devices is in providing the mechanical support to components, as well as defining the vacuum vessel boundary. Furthermore, the structural components contain the cooling infrastructure of MCF devices and ensure the required vacuum conditions. The functionality of structural materials in current fusion machines and hence, their choice, depends largely on interface properties to PFMs, blanket materials and chemical resistance to the reactive, humid or corrosive environment (Lässer et al., 2007; Zinkle and Busby, 2009). Presently, austenitic stainless steel of different types is the most widespread structural material (Kalinin et al., 2000; Barabash et al., 2007). In ITER, most of the supporting structures will be made of type 316L stainless steel (Kalinin et al., 2000). The heat sink interface material to the water-cooling infrastructure will be provided by a high strength, high conductivity copper alloy (CuCrZr) (Kalinin et al., 2000; Barabash et al., 2007).

Requirements for structural materials increase significantly in a fusion power plant due to the long required lifetimes at high temperatures in the presence of high fluxes of energetic neutrons, corrosive fluids, and large cyclic thermomechanical stresses. Superior mechanical properties and resistance to radiation induced property degradation such as embrittlement and void swelling are required to ensure acceptable reliability and component lifetimes before replacement, and low residual activation following prolonged exposure to energetic neutrons is required for safety and recycling/waste disposal considerations (Bloom, 1998). Key properties include superior elevated temperature thermo-mechanical creep-fatigue properties, resistance to neutron-induced embrittlement and stress corrosion cracking, resistance to radiation-induced dimensional changes due to irradiation creep or void swelling, and high temperature coolant corrosion resistance (Bloom et al., 2007). A particularly daunting challenge is the high levels of transmutant hydrogen (H) and helium (He) that are produced in most materials by the 14 MeV neutrons generated in the deuterium-tritium fusion reaction. These H and He gaseous transmutants tend to enhance radiation degradation processes such as low temperature embrittlement, intermediate temperature void swelling, and high temperature grain boundary embrittlement (Dai et al., 2012; Zinkle et al., 2019) dramatically. Due to the worldwide lack of a suitably intense prototypic 14 MeV neutron source (Zinkle and Möslang, 2013; Knaster et al., 2016), estimates of potential degradation rates are mainly based on limited simulation experiments and computational modeling predictions. Therefore, the structural material suite being considered for fusion power plants is quite broad.

Reduced activation ferritic-martensitic (RAFM) steels developed for fusion are the current leading candidates. These include Eurofer (Lindau et al., 2005; Möslang et al., 2005), Rusfer (Chernov et al., 2010; Rogozhkin et al., 2012; Tyumentsev et al., 2012), CLAM (Huang, 2014), F82H (Jitsukawa et al., 2002; Tanigawa et al., 2011) and JLF-1 (Kohyama et al., 1998). The historic evolution of the RAFM steel development and current status is provided e.g. in Kohyama et al. (1996); Tanigawa et al. (2017). The favorable reduced activation properties of RAFM steels is largely due to replacement of undesirable solute elements (Mo, Nb) in commercial high performance steels with similar-functioning reduced-activity elements (W, V, Ta) (Klueh and Bloom, 1985; M.R. Gilbert and Sublet, 2016). A wide variety of ultra-high-performance alternatives to the baseline RAFM steels are under intense investigation, due to concerns that higher performance properties and/or radiation resistance may be needed for next step fusion energy devices (Lindau et al., 2005; Klueh et al., 2007; Zinkle et al., 2017). These high performance alternative steels generally utilize ultra-high densities of nanoscale particles such as oxides, carbides or nitrides to improve high temperature strength and neutron radiation resistance.

Promising risk mitigation alternatives to RAFM structural materials under investigation include silicon carbide ceramic composites (Snead et al., 2007; Katoh et al., 2014) and refractory alloys such as V-4Cr-4Ti (Zinkle, 2005; Zinkle et al., 2013; Muroga et al., 2014). These structural materials offer the potential for improved thermodynamic efficiency due to $\sim$200°C–400°C higher operating range than that of RAFM steels, along with potentially improved radiation resistance compared to RAFM steels. However, the industrial experience with these materials is much less compared to that for steel production and use in engineering systems.

For the use of low-activation steels, good interface to the PFMs plays a crucial role. Due to significant difference in a wide variety of crucial parameters and, primarily, thermal conductivity and thermal expansion coefficients, direct joining of tungsten to low-activation steel is challenging (Driemeyer et al., 1999; Bachurina et al., 2018). Various joining techniques are under study, including brazing (de Prado et al., 2017; Bachurina et al., 2018), hot isostatic pressing (Driemeyer et al., 1999), field-assisted sintering technology, creation of functionally graded materials (Weber et al., 2013; Heuer et al., 2020); the use of tungsten laminates (Reiser et al., 2017) and additive manufacturing look promising. Here, the strength of the interface, the inter-diffusion of steel elements and tungsten, the phase formation and the durability under cyclic heat loads are the prime criteria for feasibility.

Tritium safety must be applied to the structural materials. The development of tritium barriers reviewed earlier in the article must suppress the undesirable diffusion of tritium in the bulk materials and prevent tritium interaction with the coolant.

Structural materials must also provide an efficient and robust interface to the cooling structure. Here, depending on coolant type, various materials or alloys with a high thermal conductivity are under investigation. For water-cooled high heat flux structural applications, the most promising are high-strength, high conductivity Cu alloys such as CuCrZr (Pintsuk et al., 2010; Barabash et al., 2011; Stork et al., 2014a; You, 2015; Richou et al., 2017, 2020) and other Cu alloys or composites are under development (You, 2015; Zinkle, 2016; Wang et al., 2020).

Different joining methods are under development (Nicholas et al., 2018) for providing robust interfaces to the heat sink materials. Joints initially created by hot isostatic pressing (HIP) face challenges, mainly due to severe thermal expansion mismatch of tungsten and heat sink materials (Barabash et al., 2000; Rigal et al., 2000). Recently, melt infiltration (Muller et al., 2017) and field-assisted sintering technology (FAST) (Galatanu et al., 2017, 2019) were applied successfully. Direct joining of tungsten to the heat sink material is another strategy of interest for divertor applications, etc. Additive manufacturing as a technique for direct joining of tungsten and the heat sink material is also under consideration (Müller et al., 2019).

Materials for magnets

Despite years of research, the magnet systems in fusion reactors are still considered to be one of the primary life-limiting components. Difficulties associated with replacing, in particular, toroidal field coils are considered a barrier to commercialization of fusion (Chislett-Mcdonald et al., 2019). The current material of choice as the superconducting material for EU-DEMO applications is niobium (Nb)—tin (Sn) alloy Nb_3Sn, but long-term reliability is an issue because of its brittleness. Nb-Ti, which is commonly used in magnetic resonance imaging machines, is a potential ductile alternative, which was recently proven applicable for advanced fusion systems with well-controlled plasma confinement requiring lower magnetic fields (Chislett-Mcdonald et al., 2019).

Meanwhile, "High temperature" (20–40 K) Rare-Earth-Ba-Cu-O (REBCO) superconducting tapes are being explored for conventional (Heller et al., 2015) and compact (spherical) fusion devices because of their ability to carry more current at higher field compared to conventional low temperature (4 K) superconductors, which is critical for compact devices (Sorbom et al., 2016; Sykes et al., 2018). These materials are immature and inherently brittle and understanding of how such materials withstand neutron irradiation damage is still largely missing. Since no ductile solution for high-field superconductors has so far been found, there is active research in devising economic engineering solutions to the problem of replacing field coils made from REBCO or otherwise (Tsui et al., 2016), which could also benefit the lower temperature options. Demountable joints are an attractive solution, allowing a modular construction of coils and making replacement easier (Sorbom et al., 2016). Soldering of the joints, e.g. using tin-based solders (Tsui et al., 2016) is the most promising solution. However, challenges are still to be overcome concerning the ability of the joints to carry currents and the reliability and repeatability of the joining process that could be required in thousands of locations in a typical fusion reactor system (Sagara et al., 2014).

Materials for inertial fusion devices

Introduction

The development of the facilities for inertial fusion is mainly focused on reaching the prime goal of attaining the ignition of D-T targets. Material development for the inertial fusion facilities is accompanying the mentioned mainstream research. Due to the different operation modes of IFE and MCF facilities, major requirements deviate significantly for these two concepts. At the same time, there are also distinct similarities. Specifically, the similarities can be noticed in requirements for the materials suggested for IFE facilities. Information on material research for IFE facilities is not as abundant as that for MCF devices. Nevertheless, the intensive pilot research conducted provides a sufficient degree of specification of the envisaged material concepts.

A schematic view of the inertial fusion facility is presented in Fig. 7 on the example of the European facility HiPER (*HiPER facility website*, 2020). Laser beams focused on the frozen D-T target with dimensions of several millimeter will ablate the outer layers of the target compressing it and causing the fusion D-T reaction reviewed in details in (Atzeni, 2021). The reaction volume is contained in a spherical reaction chamber where, as in MCF devices, the first wall will be exposed to the products of a fusion reaction. The spherical reaction chamber is the inner sphere in Fig. 7. The first wall will be fixed to the structural material, providing the mechanical support and acting as a chamber shield. The so-called final optical assembly (FOA) is contained within the second, larger spherical shield. The massive structure will hold optical tubes used to direct the powerful laser radiation beamed through the set of mirrors and lenses to the D-T target. Finally, the external cylindrical wall will encapsulate the entire volume of the inertial fusion facility. Depending on requirements and functionality the suggested materials for an IFE facility will be divided into several different classes:

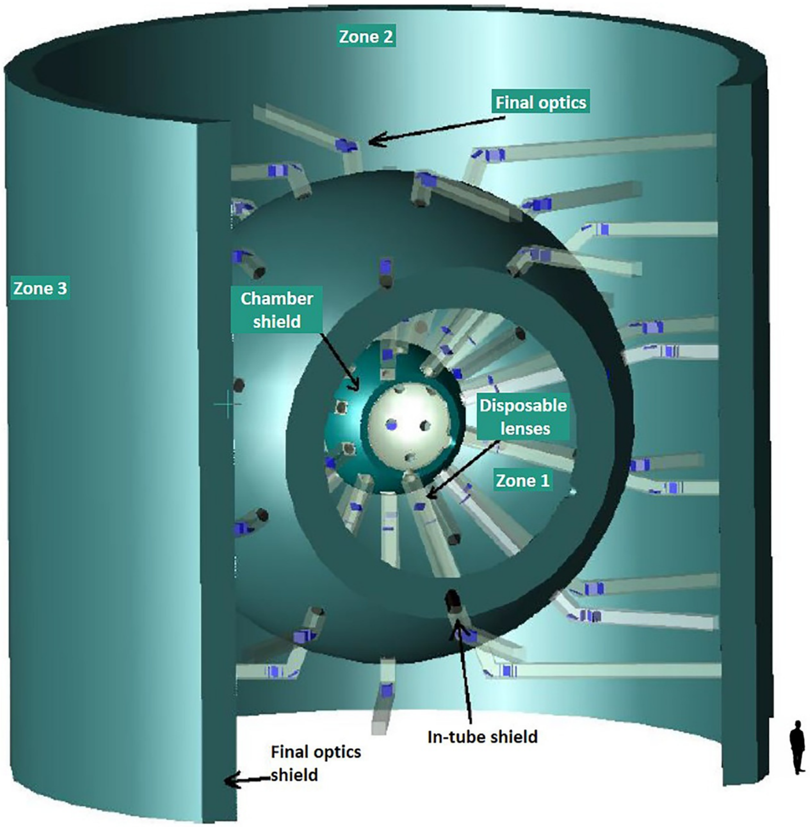

Fig. 7 A preliminary design of HiPER. Adapted from Ruiz JA, Rivera A, et al. (2011a) Materials research for HiPER laser fusion facilities: Chamber wall, structural material and final optics. *Fusion Science and Technology* 60: 565–569. doi: 10.13182/FST11-A12443.

a. First wall materials
b. Structural materials
c. Optical materials

In this sub-section we will review the main challenges and requirements for these material classes and will survey the candidate materials suggested for IFE.

Material challenges and requirements in IFE

Owing to the nature of the inertial operation, significant heat loads are expected inside the IFE facilities. Presently, the laser systems with a total power ranging from 0.5 to 1.5 megajoules will beam onto the D-T target with very short pulses of one to several nanoseconds (Chanteloup et al., 2010; Sethian et al., 2010; Ruiz et al., 2011a; Colier et al., 2013; Miquel et al., 2016; Norimatsu et al., 2017). The entire IFE facility is expected to operate with a shot frequency of several hertz. The resulting fusion energy of order of tens of megajoules, will be unloaded within the first few hundreds of nanoseconds onto the components of the first wall in the reaction chamber. The massive particle, heat and radiation loads impose a significant challenge for first wall materials. In HiPER, the expected loads to the first materials can reach about 200 GW/m^2 for the He ions originating from fusion reactions. The debris particles originating from the non-ablated remainder of D-T capsule will lead to loads of order of 40 GW/m^2 (Perlado et al., 2012) exposing the first wall for about 2 μs with a repetition rate of 1–10 Hz (Ruiz et al., 2011b).

Pulsed operation of the IFE facility will provide an additional complication. The nearly instantaneous release of a large amount of energy will impose the risk of melting and sublimation and splashing of plasma-facing materials (Norimatsu et al., 2010, 2017; Sethian et al., 2010; Ruiz et al., 2011a). Additionally, the cyclic mode of operation with a high repetition rate of shots, 24 h a day and 7 days a week in the timeframe of the envisaged 20–30 years of operation of IFE (Sethian et al., 2010; Ruiz et al., 2011a; Norimatsu et al., 2017) will significantly increase the probability of material failure as a consequence of, e.g. thermal fatigue.

Finally, intensive particle and neutron radiation originating from the D-T reactions will induce the substantial radioactivity in the components of the IFE reactor. The radiological aspects of nuclear fusion facilities are reviewed in the Chapter 01229 by N. Taylor (2021).

Material choice for IFE facilities

Plasma-facing materials

Material choice for the first wall of the reaction chamber varies strongly depending on particular design (Perlado et al., 2010, 2018; Sethian et al., 2010; Norimatsu et al., 2017). The two essential material options under consideration are:

- Solid (dry) wall
- Liquid wall

In some cases, in the course of design development there is a transition between the first wall options: a solid wall to be exchanged for a liquid wall as it was in case for the Japanese laser fusion commercial reactor project KOYO-F (Norimatsu et al., 2017). An additional options to reduce damage of the first wall includes magnetic diversion of fusion-generated ions (Sethian et al., 2010).

The choice of a solid wall usually is justified by the required robustness of the design from the beginning, based largely on the experience obtained at the MCF facilities and corresponding MCF materials testing program. Here, the reader may notice distinct similarities in material choice for IFE and MCF facilities. Because of known problems with tritium retention and formation of volatile hydrocarbons, carbon was eliminated as a candidate material for the first wall armor. Due to its natural advantages mentioned earlier, tungsten is currently being considered as the prime candidate material of the solid first wall (Juarez et al., 2010; Perlado et al., 2010, 2018; Sethian et al., 2010; Ruiz et al., 2011a). Depending on the specific design, the thickness of the first wall varies between 1 mm and 1 cm (Juarez et al., 2010; Perlado et al., 2010, 2018; Sethian et al., 2010). Alternatively, tungsten alloys or nano-structured tungsten are suggested to gain the advantage of reduced recrystallization and to relieve neutron effects (Perlado et al., 2018). It is expected that the use of tungsten with its advantageous properties will relieve the effect of thermal loads on the first wall of the envisaged ICF devices—a similar approach is followed for MCF facilities. At the same time, there is still a risk of tungsten melting, which was predicted for the particular conservative scenario in HiPER (Ruiz et al., 2011a,b). Here, the peak pulse of X-rays created after the reaction pushes the temperature of the W-armor to 3300°C within several microseconds. Detailed calculations reveal an increased risk of temperature excursions of the plasma-closest layers of the armor. Owing to the very fast response to the reaction event, the power load from the fusion burn reaches the first wall within several nanoseconds and after 1 μs up to 50% of generated power is absorbed within the first 1 μm of the tungsten wall. More realistic modeling taking into account the time evolution of the heating pulse predicts, fortunately, peak temperatures of around 1530°C (Ruiz et al., 2011a). Another essential issue is tritium permeation through the first wall material. The corresponding research is briefly reported in (Ruiz et al., 2011a). The repetitive heat loads lead to extensive crack formation and cause degradation of the thermo-mechanical properties of tungsten, as well as provoking mechanical fatigue of W (Sethian et al., 2010), as known from the MCF research (Linke et al., 2019). The corresponding studies reported for HiPER in (Ruiz et al., 2011a,b) outline the risk of cracking at the 1.5 μs after the laser shot in HiPER, when the Von Mises stress of tungsten armor exceeded 3 GPa (Blanchard and Martin, 2005). The evolving cracking can degrade the overall mechanical stability of the tungsten first wall and lead, among other consequences, to dust and debris formation.

Nevertheless, the solid wall option is treated as a relatively robust one and is incorporated in the majority of the first wall concepts. The liquid wall concepts are usually based on lithium and either represent pure Li wall solutions or the lithium-lead (Pb) combination—which is advantageous since it integrates the blanket solutions. An extensive study was reported in (Norimatsu et al., 2010, 2017). The repetitive short-pulse power loads will lead to expected effects including liquid splashing and vaporization and, eventually, ablation. The ablation of a plasma-facing 3-μm thick layer of the first wall per a single laser power pulse was predicted. The ablated materials then become split and in part strike the first wall and can subsequently re-enter the inner volume of the reaction center. Modeling predictions were experimentally validated. The propagation velocity of the ablated plume of first wall materials is of order of 1 km $\times$ s^{-1}, as detected using the Mie scattering technique (Norimatsu et al., 2010).

Important information was obtained on the nuclear decay heat in a LiPb first wall. For the LIFT test reactor (Japan) with a nominal projected fusion energy of 40 MJ per pulse operating at 1 Hz repetition rate, the resulting decay heat in the first wall still exceeds 1 MW after 10.000 h (>1 year) of operation.

Structural materials

Structural materials in IFE facilities will naturally experience, less intense power and radiation loads than the first wall. At the same time, since structural materials support the first wall armor, their long-term durability under cyclic repetitive mechanical loads and eventually, significant temperature excursions, is required. Various types of steels were therefore proposed for different IFE facilities. In the LIFT project (Japan) an F82H martensitic steel structure will hold the liquid first wall of the blanket, whereas the stainless steel SS 316 will encapsulate the cooling channels. Here, the calculations (Norimatsu et al., 2017) show a temperature periodic rise to 1500°C which will potentially endanger the steel supporting structures.

An extensive study on possible structural material options was undertaken for the HiPER project. Among others, the radiology aspects were considered. A comparative analysis of the Eurofer reduced activation steel developed for MCF (Lindau et al., 2005; Möslang et al., 2005) and the commercial SS304L steel has been performed for the standard expected HiPER operation scenarios. The scenarios comprised 100 MJ of neutron yield per shot and up to 100 shots in one burst repeated at 10 Hz, with one burst per month for 20 years. The results showed clearly that the low contact dose rate attained with SS304L reaches 1.5×10^{-5} Sv $\times$ h^{-1} in 50 years which is sufficiently low to qualify this relatively inexpensive steel for the HiPER environment. More details on the reported comparative analysis can be found in (Juarez et al., 2010).

Optical materials

By their nature, all projected IFE facilities require an extensive set of optics to guide the laser radiation to the D-T targets. The optical components comprise both the refractory and focusing optics and corresponding waveguides and supporting systems (Sethian et al., 2010). The structure of optical components is presented in Fig. 7 for the example of the HiPER facility (Ruiz et al., 2011b). In the case of optics, the radiation level and the thermomechanical loads dictate the conditions and largely govern the design of components. In HiPER, the region between the inner spherical reaction chamber and the outer spherical shield, the outer sphere in Fig. 7, is the location of the so-called disposable optics in the Final Optical Assembly (FOA). It is assumed that optical components of the FOA located within Zone 1, Fig. 7 in the course of the operation become either damaged or displaced and must be regularly exchanged. Optical components outside Zone 1 are stationary and are not supposed to be exchanged.

For optical elements in Zone 2, the prime material for the mirrors and focusing lenses is deemed to be a pure (single crystal) silica based on results of investigations summarized in (Juarez et al., 2010; Ruiz et al., 2011b). At the same time, recent calculations briefly reported in (Ruiz et al., 2011b) suggest the necessity of using cooling for at least a part of optical components. Other final optic options include grazing incidence metal mirrors (Sethian et al., 2010), similar to the choice adopted for MCF systems. For the optical tubes, several materials are under consideration including both low-activation and regular SS304L stainless steel.

Summary and outlook

In this article, we summarized the development of fusion reactor materials—one of the key pillars in attaining the ultimate goal of controlled nuclear fusion, the realization of a fusion power plant. For magnetic confinement devices: tokamaks and stellarators, we have seen the variety of processes occurring during the interactions of fusion plasmas with materials. Among them are: physical sputtering and chemical erosion, recrystallization and melting, tritium accumulation, prompt re-deposition of eroded material leading to the dust formation, and significant changes imposed by plasma particles and radiation on the microstructure and surface of plasma-facing materials. The majority of these processes are also expected to occur in inertial confinement devices. The processes of plasma-material interactions have imposed severe requirements on the candidate material concepts. It is interesting to see a kind of "loop" in the development of fusion materials from metals widely spread in fusion facilities in 1970s, to the light, carbon-based materials and beryllium dominant until 2000s and then, a return to the metals nowadays. Advanced plasma control scenarios, and improved plasma heating knowledge have largely contributed to this return to high-Z refractory metals, such as tungsten. However, achievements were scored not on the plasma side only. The development of new material concepts, such as fiber components, suitable as plasma-facing materials, and significantly advanced engineering of components, have contributed to the return of the high-Z metal option, an option which was even hard to imagine for fusion devices before.

Presently, we are witnessing the next, remarkable stage in the development of plasma-facing materials—the creation of the advanced, entirely novel, high-Z material concepts and alloys. Their features are unique: from the capability of handling enormous heat loads without serious damage, to the resistance to cracking and recrystallization and even a capability to adapt the material properties to the environment—an unbelievable set of properties is now in our hands. A liquid first wall and divertor—options that looked like a fantasy before, are now becoming a reality and we see first design solutions for the liquid metal components for a future fusion power plant.

Material development for the inertial fusion facilities is largely harnessing the intensive synergetic research results gained for magnetic confinement fusion devices. As for the first wall of the reaction chamber, two primary concepts are presently under consideration. The so-called "solid" wall is planned to be built either from pure tungsten or from the advanced nano-grain tungsten or tungsten alloys. Alternatively, for several IFE reactor concepts, a self-cooling lithium-based liquid wall has been suggested. Here, issues may arise potentially with the recycling of liquid material and with the stability of a liquid under cyclic high thermal, mechanical and radiation loads. The advantages of a liquid wall are the ability to act as a blanket for tritium breeding and the absence of a requirement for active cooling.

Optical materials for IFE facilities, such as like mirrors, frequency multipliers and focusing lenses will largely rely on established material concepts. Presently, it is planned to use pure silica for all these elements, although adjustments may become necessary for optic components located in final optical assembly.

Optical systems of the MCF facilities will rely on mirror-based reflective optics. Here, the use of unique, highly reflective material concepts, such as single crystal molybdenum and rhodium for diagnostic mirrors—with their unprecedented capability to preserve the reflectivity under plasma sputtering, have opened the way for mirror-based diagnostics which can last for the entire lifetime of future MCF devices. The dedicated facilities for mirror surface recovery, including in situ mirror cleaning and calibration systems, will support the retention of high mirror performance.

Development of efficient and reliable blanket technology represents technological, physics and engineering challenges. Several promising concepts are under development and their simultaneous testing in the ITER test blanket modules is foreseen as a part of the R&D and qualification program.

Last, but not least, exciting progress has been achieved in structural materials. Whereas, conditions in inertial facilities luckily allow the use of conventional martensitic steel, the creation of the entire class of the reduced activation steels including Eurofer, Rusfer, CLAM, F82H—has dramatically changed the R&D and opened the way to their unmatched functionality in magnetic fusion devices.

Of course, as we have seen, the material choice and especially, the realization of the components for a fusion power plant are still far from the final stage. Significant remaining challenges include the suppression and effective control of transient power and particle loads in MCF and IFE facilities and the long-term degradation of materials. The design of MCF power plants will also benefit from the development of ductile, robust superconducting materials, or from the reliable engineering solutions for existing superconducting materials, an issue which will be addressed by ITER operation.

In a fusion power plant, materials will have to withstand, and retain their functionality under a very high fluence of highly energetic 14 MeV neutrons—and neutron-resistant material solutions must still be thoroughly tested in the burning plasma environment. However, with the solid portfolio of advanced materials developed to date, and considering the impressive progress already made on fusion materials, a significant basis exists for the development of the materials required for construction of a fusion power plant and finally, for the production of fusion—based electricity to the grid.

References

Abdou M, Morley NB, et al. (2015) Blanket/first wall challenges and required R&D on the pathway to DEMO. *Fusion Engineering and Design* 100: 2–43. https://doi.org/10.1016/j.fusengdes.2015.07.021.

Antusch S, et al. (2011) Powder Injection Molding—An innovative manufacturing method for He-cooled DEMO divertor components. *Fusion Engineering and Design* 86(9–11): 1575–1578. https://doi.org/10.1016/j.fusengdes.2011.01.009.

Artsimovich LA (1972) Tokamak devices. *Nuclear Fusion* 12(2): 215–252. https://doi.org/10.1088/0029-5515/12/2/012.

Atsumi H, et al. (1985) Thermal desorption of deuterium and helium from ion irradiated graphite. *Journal of Nuclear Materials* 133–134: 268–271. https://doi.org/10.1016/0022-3115(85)90148-5.

Atzeni S (2021) In: Greenspan E and Campbell DJ (eds.) *This Encyclopedia*. Elsevier B.V.

Aymar R (2002) ITER status, design and material objectives. *Journal of Nuclear Materials* 307–311(1): 1–9. https://doi.org/10.1016/S0022-3115(02)00937-6.

Bachurina D, et al. (2018) Joining of tungsten with low-activation ferritic–martensitic steel and vanadium alloys for demo reactor. *Nuclear Materials and Energy* 15: 135–142. https://doi.org/10.1016/j.nme.2018.03.010.

Baldwin MJ and Doerner RP (2008) Helium induced nanoscopic morphology on tungsten under fusion relevant plasma conditions. *Nuclear Fusion* 48(3). https://doi.org/10.1088/0029-5515/48/3/035001.

Barabash V, et al. (1999) Armour materials for the ITER plasma facing components. *Physica Scripta* T81(1): 74. https://doi.org/10.1238/physica.topical.081a00074.

Barabash V, et al. (2000) Armor and heat sink materials joining technologies development for ITER plasma facing components. *Journal of Nuclear Materials*. https://doi.org/10.1016/S0022-3115(00)00120-3.

Barabash V, et al. (2007) Materials challenges for ITER—Current status and future activities. *Journal of Nuclear Materials* 367–370A: 21–32. https://doi.org/10.1016/j.jnucmat.2007.03.017. (SPEC. ISS.).

Barabash VR, et al. (2011) Specification of CuCrZr alloy properties after various thermo-mechanical treatments and design allowables including neutron irradiation effects. *Journal of Nuclear Materials* 417(1–3): 904–907. https://doi.org/10.1016/j.jnucmat.2010.12.158.

Baylor LR, et al. (2012) Experimental demonstration of high frequency ELM pacing by pellet injection on DIII-D and extrapolation to ITER. In: Proceedings of the 24th IAEA Fusion Energy Conference, p. 56. International Atomic Energy Agency (IAEA). Available at: http://www-pub.iaea.org/MTCD/Meetings/PDFplus/2012/cn197/cn197_Programme.pdf.

Bazylev B, et al. (2011) Numerical simulations of tungsten melt layer erosion caused by J x B force at TEXTOR. *Physica Scripta* T145: 14054. https://doi.org/10.1088/0031-8949/2011/t145/014054.

Bazylev B, et al. (2014) *MEMOS code validation on JET transient tungsten melting experiments*. EUROfusion report EFDA–JET–CP(14)01/06 Culham: EUROfusion.

Bergsåker H, et al. (2011) Studies of mobile dust in scrape-off layer plasmas using silica aerogel collectors. *Journal of Nuclear Materials* 415(1). https://doi.org/10.1016/j.jnucmat.2011.01.052.

Bernard E, et al. (2015) Temperature impact on W surface exposed to He plasma in LHD and its consequences for the material properties. *Journal of Nuclear Materials* 463: 316–319. https://doi.org/10.1016/j.jnucmat.2014.11.041.

Biel W, et al. (2019) Diagnostics for plasma control—From ITER to DEMO. *Fusion Engineering and Design* 146: 465–472. https://doi.org/10.1016/j.fusengdes.2018.12.092.

Blanchard JP and Martin CJ (2005) Thermomechanical effects in a laser IFE first wall. *Journal of Nuclear Materials* 347(3): 192–206. https://doi.org/10.1016/j.jnucmat.2005.08.007.

Bloom EE (1998) The challenge of developing structural materials for fusion power systems. *Journal of Nuclear Materials* 258–263(Part 1 A): 7–17. https://doi.org/10.1016/S0022-3115(98)00352-3.

Bloom EE, et al. (2007) Critical questions in materials science and engineering for successful development of fusion power. *Journal of Nuclear Materials* 367–370A: 1–10. https://doi.org/10.1016/j.jnucmat.2007.02.007. (SPEC. ISS.).

Boccaccini LV (2013) Progress in EU blanket technology. *Fusion Science and Technology*. 64: pp. 615–622. Taylor & Francis. https://doi.org/10.13182/FST13-A19160.

Boccaccini LV (2021) In: Greenspan E and Campbell DJ (eds.) *This Encyclopedia*. Elsevier B.V.

Boccaccini LV, et al. (2004) Materials and design of the European DEMO blankets. *Journal of Nuclear Materials* 329–333(1–3): 148–155. https://doi.org/10.1016/j.jnucmat.2004.04.125.

Bohmeyer W, et al. (2005) Transport and deposition of injected hydrocarbons in plasma generator PSI-2. *Journal of Nuclear Materials* 337–339(1–3): 89–93. https://doi.org/10.1016/j.jnucmat.2004.10.107. SPEC. ISS.

Bonnin X, et al. (2017) ITER divertor plasma response to time-dependent impurity injection. *Nuclear Materials and Energy* 12: 1100–1105. https://doi.org/10.1016/j.nme.2017.03.010.

Borodin D, et al. (2011) ERO code benchmarking of ITER first wall beryllium erosion/re-deposition against LIM predictions. *Physica Scripta* T145. https://doi.org/10.1088/0031-8949/2011/T145/014008.

Borodin D, et al. (2019) Improved ERO modelling of beryllium erosion at ITER upper first wall panel using JET-ILW and PISCES-B experience. *Nuclear Materials and Energy* 19: 510–515. https://doi.org/10.1016/j.nme.2019.03.016.

Breton C, De Michelis C, and Mattioli M (1976) Radiation losses from oxygen and iron impurities in a high-temperature plasma. *Nuclear Fusion* 16(6): 891–899. https://doi.org/10.1088/0029-5515/16/6/001.

Brezinsek S, et al. (2013) Fuel retention studies with the ITER-Like Wall in JET. *Nuclear Fusion* 53(8): 83023. https://doi.org/10.1088/0029-5515/53/8/083023.

Brezinsek S, Coenen JWW, et al. (2017a) Plasma-wall interaction studies within the EUROfusion consortium: Progress on plasma-facing components development and qualification. *Nuclear Fusion* 57(11). https://doi.org/10.1088/1741-4326/aa796e.

Brezinsek S, Hakola A, et al. (2017b) Surface modification of He pre-exposed tungsten samples by He plasma impact in the divertor manipulator of ASDEX upgrade. *Nuclear Materials and Energy* 12: 575–581. https://doi.org/10.1016/j.nme.2016.11.002.

Brooks JN, et al. (2014) Scientific and computational challenges in coupled plasma edge/plasma-material interactions for fusion tokamaks. *Contributions to Plasma Physics* 54(4–6): 329–340. https://doi.org/10.1002/ctpp.201410014.

Buzi L, et al. (2014) Influence of particle flux density and temperature on surface modifications of tungsten and deuterium retention. *Journal of Nuclear Materials* 455(1–3). https://doi.org/10.1016/j.jnucmat.2014.06.059.

Carpentier S, et al. (2011) Modelling of beryllium erosion-redeposition on ITER first wall panels. *Journal of Nuclear Materials*. https://doi.org/10.1016/j.jnucmat.2010.10.081.

Cenedese A and Sartori F (2004) Plasma position and current control management at JET. Proceedings of the IEEE Conference on Decision and Control, vol. 5, pp. 4628–4633. IEEE. https://doi.org/10.1109/CDC.2003.1272293.

Chanteloup JC, et al. (2010) Multi kJ level laser concepts for HiPER facility. *Journal of Physics: Conference Series* 244(1). https://doi.org/10.1088/1742-6596/244/1/012010.

Chernov VM, et al. (2010) *Heat-resistant ferritic-martensitic steel RUSFER-EK-181 (Fe-12Cr-2W-V-Ta-B) for fusion power reactor*. International Atomic Energy Agency (IAEA). Available at: http://www-pub.iaea.org/MTCD/Meetings/PDFplus/2010/cn180/cn180_BookOfAbstracts.pdf.

Chih YK, et al. (2011) Surface modification of hollow carbon fibres using plasma treatment. *Surface Engineering* 27(8): 623–626. https://doi.org/10.1179/026708410X12786785573391.

Chislett-Mcdonald SBL, Surrey E, and Hampshire DP (2019) Could high H 98-factor commercial tokamak power plants use Nb-Ti toroidal field coils? *IEEE Transactions on Applied Superconductivity* 29(5): 1–5. https://doi.org/10.1109/TASC.2019.2896402.

Coenen JW (2020) Fusion materials development at Forschungszentrum Jülich. *Advanced Engineering Materials* 22(6): 1–15. https://doi.org/10.1002/adem.201901376.

Coenen JW, et al. (2011) Analysis of tungsten melt-layer motion and splashing under tokamak conditions at {TEXTOR}. *Nuclear Fusion* 51(8): 83008. https://doi.org/10.1088/0029-5515/51/8/083008.

Coenen JW, et al. (2014) Liquid metals as alternative solution for the power exhaust of future fusion devices: Status and perspective. *Physica Scripta* T159. https://doi.org/10.1088/0031-8949/2014/T159/014037.

Coenen JW, et al. (2015) ELM-induced transient tungsten melting in the JET divertor. *Nuclear Fusion* 55(2): 23010. https://doi.org/10.1088/0029-5515/55/2/023010.

Coenen JWW, et al. (2016) Materials for DEMO and reactor applications—Boundary conditions and new concepts. *Physica Scripta* T167. https://doi.org/10.1088/0031-8949/2016/T167/014002.

Coenen JW, et al. (2017) Transient induced tungsten melting at the Joint European Torus (JET). *Physica Scripta* T170: 14013. https://doi.org/10.1088/1402-4896/aa8789.

Coenen JW, et al. (2018) Improved pseudo-ductile behavior of powder metallurgical tungsten short fiber-reinforced tungsten (Wf/W). *Nuclear Materials and Energy*. https://doi.org/10.1016/j.nme.2018.05.001.

Colier J, et al. (2013) HiPER Preparatory Phase Final Report.

Costley AE (2019) Towards a compact spherical tokamak fusion pilot plant. *Philosophical Transactions of the Royal Society A: Mathematical, Physical and Engineering Sciences* 377(2141). https://doi.org/10.1098/rsta.2017.0439.

Costley AE, et al. (2001) ITER R&D: Auxiliary systems: Plasma diagnostics. *Fusion Engineering and Design* 55(2–3): 331–346. https://doi.org/10.1016/S0920-3796(01)00200-9.

Costley AE, et al. (2005) Technological challenges of ITER diagnostics. *Fusion Engineering and Design* 74(1–4): 109–119. https://doi.org/10.1016/j.fusengdes.2005.08.026.

Dai Y, Odette GR, and Yamamoto T (2012) The effects of helium in irradiated structural alloys. In: *Comprehensive Nuclear Materials*, 1st edn. Elsevier Inc.https://doi.org/10.1016/B978-0-08-056033-5.00006-9

de Prado J, et al. (2017) Development of W-composites/{EUROFER} brazed joints for the first wall component of future fusion reactors. *Physica Scripta* T170: 14026. https://doi.org/10.1088/1402-4896/aa8bda.

De Temmerman G, et al. (2008) An empirical scaling for deuterium retention in co-deposited beryllium layers. *Nuclear Fusion* 48(7). https://doi.org/10.1088/0029-5515/48/7/075008.

De Temmerman G, Doerner RP, and Pitts RA (2019) A growth/annealing equilibrium model for helium-induced nanostructure with application to ITER. *Nuclear Materials and Energy* 19: 255–261. https://doi.org/10.1016/j.nme.2019.01.034.

De Tommasi G (2019) Plasma magnetic control in Tokamak Devices. *Journal of Fusion Energy* 38(3): 406–436. https://doi.org/10.1007/s10894-018-0162-5.

Dejarnac R and Gunn JP (2007) Kinetic calculation of plasma deposition in castellated tile gaps. *Journal of Nuclear Materials* 363–365(1–3): 560–564. https://doi.org/10.1016/j.jnucmat.2006.12.055.

Ding F, et al. (2014) Overview of plasma-material interaction experiments on EAST employing MAPES. *Journal of Nuclear Materials* 455(1). https://doi.org/10.1016/j.jnucmat.2014.09.017.

Dittmar T, et al. (2011) Deuterium inventory in tore supra (DITS): 2nd post-mortem analysis campaign and fuel retention in the gaps. *Journal of Nuclear Materials*. https://doi.org/10.1016/j.jnucmat.2010.11.075.

Doerner RP, Baldwin MJ, and Nishijima D (2014) Plasma-induced morphology of beryllium targets exposed in PISCES-B. *Journal of Nuclear Materials* 455(1): 1–4. https://doi.org/10.1016/j.jnucmat.2014.02.010.

Donné AJH, et al. (2007) Chapter 7: Diagnostics. *Nuclear Fusion* 47(6). https://doi.org/10.1088/0029-5515/47/6/S07.

Donne AJH, et al. (2021) Chapter 01217. In: Greenspan E and Campbell DJ (eds.) *This Encyclopedia*. Elsevier B.V.

Driemeyer DE, et al. (1999) Development of direct HIP-bonding processes for tungsten-brush armor joining. In: *18th IEEE/NPSS Symposium on Fusion Engineering. Symposium Proceedings (Cat. No.99CH37050)* 369–372. https://doi.org/10.1109/FUSION.1999.849858.

Duffy DM (2009) Modeling plasma facing materials for fusion power. *Materials Today* 12(11): 38–44. https://doi.org/10.1016/S1369-7021(09)70297-4.

Eckstein W, et al. (1993) Sputtering data. Report of IPP Garching IPP 9/82. Garching, Germany.

Eldon D, et al. (2017) Controlling marginally detached divertor plasmas. *Nuclear Fusion* 57(6): 66039. https://doi.org/10.1088/1741-4326/aa6b16.

Eren B, et al. (2011) Reflective metallic coatings for first mirrors on ITER. *Fusion Engineering and Design* 86(9–11). https://doi.org/10.1016/j.fusengdes.2010.12.038.

Evans TE (2013) ELM mitigation techniques. *Journal of Nuclear Materials* 438: S11–S18. https://doi.org/10.1016/j.jnucmat.2013.01.283.

Evtikhin VA, Lyublinsky IE, et al. (2002a) Lithium divertor concept and results of supporting experiments. *Plasma Physics and Controlled Fusion* 44: 955.

Evtikhin VA, Vertkov AV, et al. (2002b) Research of lithium capillary-pore systems for fusion reactor plasma facing components. *Journal of Nuclear Materials* 307–311(2): 1664–1669. https://doi.org/10.1016/S0022-3115(02)01132-7.

Federici G, et al. (2001) Plasma-material interactions in current tokamaks and their implications for next step fusion reactors. *Nuclear Fusion* 41(12): 1967–2137. https://doi.org/10.1088/0029-5515/41/12/218.

Federici G, et al. (2017) European DEMO design strategy and consequences for materials. *Nuclear Fusion* 57(9): 92002. https://doi.org/10.1088/1741-4326/57/9/092002.

Federici G, et al. (2018) DEMO design activity in Europe: Progress and updates. *Fusion Engineering and Design* 136: 729–741. https://doi.org/10.1016/j.fusengdes.2018.04.001.

Federici G, et al. (2019) An overview of the EU breeding blanket design strategy as an integral part of the DEMO design effort. *Fusion Engineering and Design* 141: 30–42. https://doi.org/10.1016/j.fusengdes.2019.01.141.

Fedorov AV, et al. (2016) Post irradiation characterization of beryllium and beryllides after high temperature irradiation up to 3000 appm helium production in HIDOBE-01. *Fusion Engineering and Design* 102: 74–80. https://doi.org/10.1016/j.fusengdes.2015.10.024.

Firdaouss M, et al. (2017) Overview of the different processes of tungsten coating implemented into WEST tokamak. *Fusion Engineering and Design* 124: 207–210. https://doi.org/10.1016/j.fusengdes.2017.02.087.

Flament T, et al. (1992) Compatibility of materials in fusion first wall and blanket structures cooled by liquid metals. *Journal of Nuclear Materials* 191–194: 132–138. https://doi.org/10.1016/S0022-3115(09)80020-2.

Galatanu M, et al. (2017) Cu-based composites as thermal barrier materials in DEMO divertor components. *Fusion Engineering and Design* 124: 1131–1134. https://doi.org/10.1016/j.fusengdes.2017.02.031.

Galatanu M, et al. (2019) Development of W-monoblock divertor components with embedded thermal barrier interfaces. *Fusion Engineering and Design* 146: 1351–1354. https://doi.org/10.1016/j.fusengdes.2019.02.074.
Galvao R (2021) In: Greenspan E and Campbell DJ (eds.) *This Encyclopedia*. Elsevier.
García-Rosales C, et al. (2014) Oxidation behaviour of bulk W-Cr-Ti alloys prepared by mechanical alloying and HIPing. *Fusion Engineering and Design* 89(7–8): 1611–1616. https://doi.org/10.1016/j.fusengdes.2014.04.057.
Gasparyan Y, Efimov V, and Bystrov K (2016) Helium concentration measurement in tungsten fuzz-like nanostructures by means of thermal desorption spectroscopy. *Nuclear Fusion* 56(5): 18–21. https://doi.org/10.1088/0029-5515/56/5/054002.
Gelles DS, et al. (1994) Radiation effects in beryllium used for plasma protection. *Journal of Nuclear Materials* 212–215(1): 29–38. https://doi.org/10.1016/0022-3115(94)90030-2.
Giancarli LM, et al. (2012) Overview of the ITER TBM Program. *Fusion Engineering and Design* 87(5–6): 395–402. https://doi.org/10.1016/j.fusengdes.2011.11.005.
Gilbert MR and Sublet JC (2016) *Handbook of Activation, Transmutation, and Radiation Damage Properties of the Elements Simulated Using FISPACT-II & TENDL-2015 for Magnetic Fusion Plants*. CCFE.
Gilbert MR and Sublet JC (2017) Scoping of material response under DEMO neutron irradiation: Comparison with fission and influence of nuclear library selection. *Fusion Engineering and Design* 125: 299–306. https://doi.org/10.1016/j.fusengdes.2017.06.016.
Gilbert MR, et al. (2012) An integrated model for materials in a fusion power plant: Transmutation, gas production, and helium embrittlement under neutron irradiation. *Nuclear Fusion* 52(8). https://doi.org/10.1088/0029-5515/52/8/083019.
Grisolia C, et al. (2009) From eroded material to dust: An experimental evaluation of the mobilised dust production in Tore Supra. *Journal of Nuclear Materials* 390–391(1): 53–56. https://doi.org/10.1016/j.jnucmat.2009.01.045.
Gruber O, et al. (2009) Compatibility of ITER scenarios with full tungsten wall in ASDEX upgrade. *Nuclear Fusion* 49(11): 115014. https://doi.org/10.1088/0029-5515/49/11/115014.
Guo W, et al. (2018) Retarded recrystallization of helium-exposed tungsten. *Nuclear Fusion* 58(10): 106011. https://doi.org/10.1088/1741-4326/aad2b0.
Haasz AA, et al. (1987) Synergistic methane formation on pyrolytic graphite due to combined H+ ion and H0 atom impact. *Journal of Nuclear Materials* 145–147(C): 412–416. https://doi.org/10.1016/0022-3115(87)90371-0.
Hayashi T, et al. (2006) Safety handling characteristics of high-level tritiated water. *Fusion Engineering and Design* 81(8): 1365–1369. https://doi.org/10.1016/j.fusengdes.2005.09.062.
Heller R, et al. (2015) Conceptual design improvement of a toroidal field coil for EU DEMO using high temperature superconductors. In: *Report at 24th International Conference on Magnet Technology (MT 2015)* . Seoul, Korea, October 18–23, 2015.
Herrmann A, et al. (2017) Experiences with a solid tungsten divertor in ASDEX Upgrade. *Nuclear Materials and Energy* 12: 205–209. https://doi.org/10.1016/j.nme.2017.03.001.
Heuer S, et al. (2020) Overview of challenges and developments in joining tungsten and steel for future fusion reactors. *Physica Scripta* T171: 14028. https://doi.org/10.1088/1402-4896/ab47a4.
Hill DN (1997) A review of ELMs in divertor tokamaks. *Journal of Nuclear Materials* 241–243: 182–198. https://doi.org/10.1016/S0022-3115(97)80039-6.
HiPER facility website (2020) http://www.hiper-laser.org/.
Hirai T, et al. (2016) Use of tungsten material for the ITER divertor. *Nuclear Materials and Energy* 9: 616–622. https://doi.org/10.1016/j.nme.2016.07.003.
Hodgson E (1998) Radiation problems and testing of ITER diagnostic components. In: Stott PE, Gorini G, and Prandoni P (eds.) *Diagnostics for Experimental Thermonuclear Fusion Reactors 2*. Boston, MA: Springer Available at: https://books.google.de/books?id=9aGhhrMU-lkC.
Hollmann E, et al. (2011) Plasma–surface interactions during tokamak disruptions and rapid shutdowns. *Journal of Nuclear Materials* 415. https://doi.org/10.1016/j.jnucmat.2010.10.009.
Hong S-H, et al. (2014) Preliminary test results on tungsten tile with castellation structures in KSTAR. *Fusion Engineering and Design* 89(7–8). https://doi.org/10.1016/j.fusengdes.2014.01.033.
Hong S-H, et al. (2015) Toward tungsten plasma-facing components in kstar: Research on plasma-metal wall interaction. *Fusion Science and Technology* 68(1). https://doi.org/10.13182/FST14-897.
Houben A, Rasinski M, and Linsmeier C (2020) Hydrogen permeation in fusion materials and the development of tritium permeation barriers. *Plasma and Fusion Research* 15: 2405016. https://doi.org/10.1585/pfr.15.2405016.
Huang Q (2014) Development status of CLAM steel for fusion application. *Journal of Nuclear Materials* 455(1): 649–654. https://doi.org/10.1016/j.jnucmat.2014.08.055.
IFMIF DONES Facility (2020) IFMIF DONES Facility. Available at: https://ifmifdones.org/.
Igitkhanov Y, et al. (2013) *Design strategy for the PFC in DEMO reactor*. KIT Scientific Report 7637 Karlsruhe: Karlsruhe Institute of Technology.
Ioffe MS (1965) Magnetic traps. In: *Plasma Physics*, p. 420. Vienna: International Atomic Energy Agency. Available at: http://articles.adsabs.harvard.edu//full/1965plph.conf..421I/0000421.000.html.
ITER Fusion Reactor Website (2020) Official website of ITER fusion reactor. Available at: www.iter.org.
Jacob W (2005) Redeposition of hydrocarbon layers in fusion devices. *Journal of Nuclear Materials* 337–339(1–3): 839–846. https://doi.org/10.1016/j.jnucmat.2004.10.035. SPEC. ISS.
Jasper B, et al. (2015) Powder metallurgical tungsten fiber-reinforced tungsten. *Materials Science Forum*. https://doi.org/10.4028/www.scientific.net/MSF.825-826.125.
Jasper B, et al. (2016) Behavior of tungsten fiber-reinforced tungsten based on single fiber push-out study. *Nuclear Materials and Energy*. https://doi.org/10.1016/j.nme.2016.04.010.
Jenko F (2021) In: Greenspan E and Campbell DJ (eds.) *This Encyclopedia*. Elsevier B.V.
Jitsukawa S, et al. (2002) Development of an extensive database of mechanical and physical properties for reduced-activation martensitic steel F82H. *Journal of Nuclear Materials* 307–311(1): 179–186. https://doi.org/10.1016/S0022-3115(02)01075-9.
Juarez L, Sanz J, and Perlado JM (2010) Overview on neutronics, safety and radiological protection of HiPER facility. In: Proceedings of the 23 IAEA Fusion Energy Conference, Vienna: International Atomic Energy Agency IFE/P6-22: https://www-pub.iaea.org/mtcd/meetings/PDFplus/2010/cn180/cn180_papers/ife_p6-22.pdf.
Juslin N and Wirth BD (2013) Molecular dynamics simulation of the effect of sub-surface helium bubbles on hydrogen retention in tungsten. *Journal of Nuclear Materials* 438: S1221–S1223. https://doi.org/10.1016/j.jnucmat.2013.01.270.
Kajita S, et al. (2009) Formation process of tungsten nanostructure by the exposure to helium plasma under fusion relevant plasma conditions. *Nuclear Fusion* 49(9). https://doi.org/10.1088/0029-5515/49/9/095005.
Kajita S, et al. (2011) TEM observation of the growth process of helium nanobubbles on tungsten: Nanostructure formation mechanism. *Journal of Nuclear Materials* 418(1): 152–158. https://doi.org/10.1016/j.jnucmat.2011.06.026.
Kalinin G, et al. (2000) Assessment and selection of materials for ITER in-vessel components. *Journal of Nuclear Materials* 283–287: 10–19. https://doi.org/10.1016/S0022-3115(00)00305-6.
Kantor M, et al. (2013) Characterization of dust particles in the TEXTOR tokamak with Thomson scattering diagnostic. *Journal of Nuclear Materials* 438: S711. https://doi.org/10.1016/j.jnucmat.2013.01.150.
Katoh Y, et al. (2014) Continuous SiC fiber, CVI SiC matrix composites for nuclear applications: Properties and irradiation effects. *Journal of Nuclear Materials* 448(1–3): 448–476. https://doi.org/10.1016/j.jnucmat.2013.06.040.
Kesternich W and Ullmaier H (2003) Mechanical properties and microstructure of helium-implanted beryllium. *Journal of Nuclear Materials* 312: 212–223. https://doi.org/10.1016/S0022-3115(02)01637-9.

Khripunov BI, et al. (2001) Experimental study of lithium target under high power load. *Journal of Nuclear Materials* 290–293: 201. https://doi.org/10.1016/S0022-3115(00)00433-5.
Khripunov BI, et al. (2003) Liquid lithium surface research and development. *Journal of Nuclear Materials* 313–316. https://doi.org/10.1016/S0022-3115(02)01450-2.
Kirschner A (2020) PWI processes. Private communications.
Kirschner A, et al. (2016) Modelling of impurity transport and plasma–wall interaction in fusion devices with the ERO code: Basics of the code and examples of application. *Contributions to Plasma Physics* 56(6–8): 622–627. https://doi.org/10.1002/ctpp.201610014.
Klein F, Wegener T, Litnovsky A, Rasinski M, Tan XY, Schmitz J, et al. (2018a) On oxidation resistance mechanisms at 1273 K of tungsten-based alloys containing chromium and yttria. *Metals* 8(7): 488. https://doi.org/10.3390/met8070488.
Klein F, Wegener T, Litnovsky A, Rasinski M, Tan XY, Gonzalez-Julian J, et al. (2018b) Oxidation resistance of bulk plasma-facing tungsten alloys. *Nuclear Materials and Energy* 15: 226–231. https://doi.org/10.1016/j.nme.2018.05.003.
Klimov N, et al. (2011) Experimental study of PFCs erosion and eroded material deposition under ITER-like transient loads at the plasma gun facility QSPA-T. *Journal of Nuclear Materials* 415(1): 59–64. https://doi.org/10.1016/j.jnucmat.2011.01.013.
Klueh RL and Bloom EE (1985) The development of ferritic steels for fast induced-radioactivity decay for fusion reactor applications. *Nuclear Engineering and Design* 2(3): 383–389. https://doi.org/10.1016/0167-899X(85)90026-6.
Klueh RL, Hashimoto N, and Maziasz PJ (2007) New nano-particle-strengthened ferritic/martensitic steels by conventional thermo-mechanical treatment. *Journal of Nuclear Materials* 367–370A: 48–53. https://doi.org/10.1016/j.jnucmat.2007.03.001. SPEC. ISS.
Knaster J, Moeslang A, and Muroga T (2016) Materials research for fusion. *Nature Physics* 12(5): 424–434. https://doi.org/10.1038/NPHYS3735.
Koch F and Bolt H (2007) Self passivating W-based alloys as plasma facing material for nuclear fusion. *Physica Scripta, T* T128: 100–105. https://doi.org/10.1088/0031-8949/2007/T128/020.
Koch F, Köppl S, and Bolt H (2009) Self passivating W-based alloys as plasma-facing material. *Journal of Nuclear Materials* 386–388C: 572–574. https://doi.org/10.1016/j.jnucmat.2008.12.179.
Koch F, et al. (2011) Oxidation behaviour of silicon-free tungsten alloys for use as the first wall material. *Physica Scripta, T* T145: 014019. https://doi.org/10.1088/0031-8949/2011/T145/014019.
Kohyama A, et al. (1996) Low activation ferritic and martensitic steels for fusion applications. *Journal of Nuclear Materials* 233–237(1): 138–147.
Kohyama A, et al. (1998) Production of low activation steel; JLF-1, large heats—Current status and future plan. *Journal of Nuclear Materials* 258–263(2B): 1319–1323. https://doi.org/10.1016/S0022-3115(98)00198-6.
Koivuranta S, et al. (2013) Post-mortem measurements of fuel retention at JET in 2007-2009 experimental campaign. *Journal of Nuclear Materials* 438. https://doi.org/10.1016/j.jnucmat.2013.01.156.
Komm M, et al. (2011) Particle-in-cell simulations of plasma interaction with shaped and unshaped gaps in TEXTOR. *Plasma Physics and Controlled Fusion* 53(11). https://doi.org/10.1088/0741-3335/53/11/115004.
Konings RJM, et al. (ed.) (2012) *Comprehensive Nuclear Materials*, 1st edn. Amsterdam: Elsevier Ltd. Available at: https://www.sciencedirect.com/referencework/9780080560335/comprehensive-nuclear-materials#book-info.
Krasheninnikov SI (2011) Viscoelastic model of tungsten "fuzz" growth. *Physica Scripta* T145. https://doi.org/10.1088/0031-8949/2011/T145/014040.
Krasheninnikov SI, et al. (2005) On dust in tokamak edge plasmas. *Journal of Nuclear Materials* 337–339(1–3): 65–68. https://doi.org/10.1016/j.jnucmat.2004.09.031. SPEC. ISS.
Krasheninnikov SI, et al. (2008) Recent progress in understanding the behavior of dust in fusion devices. *Plasma Physics and Controlled Fusion* 50(12). https://doi.org/10.1088/0741-3335/50/12/124054.
Krasikov Y, et al. (2011) Development of design options for the port plug components of the ITER core CXRS diagnostic. *Fusion Engineering and Design* 86(9–11): 2055–2059. https://doi.org/10.1016/j.fusengdes.2011.01.086.
Kreter A, et al. (2014) Erosion, formation of deposited layers and fuel retention for beryllium under the influence of plasma impurities. *Physica Scripta* T159: 14039. https://doi.org/10.1088/0031-8949/2014/t159/014039.
Krieger K, et al. (2007) Formation of deuterium-carbon inventories in gaps of plasma facing components. *Journal of Nuclear Materials* 363–365(1–3). https://doi.org/10.1016/j.jnucmat.2007.01.155.
Krieger K, et al. (2018) Experiments on transient melting of tungsten by ELMs in ASDEX upgrade. *Nuclear Fusion* 58(2). https://doi.org/10.1088/1741-4326/aa9a05.
Krimmer A, et al. (2013) Design and testing of secondary mirrors for the core CXRS diagnostic system in ITER. *Fusion Engineering and Design* 88(9): 2021–2024. https://doi.org/10.1016/j.fusengdes.2013.02.010.
Kurishita H, et al. (2010) Development of re-crystallized W–1.1%TiC with enhanced room-temperature ductility and radiation performance. *Journal of Nuclear Materials* 398: 87–92. https://doi.org/10.1016/j.jnucmat.2009.10.015.
Lang PT, et al. (2013) ELM control strategies and tools: Status and potential for ITER. *Nuclear Fusion* 53(4). https://doi.org/10.1088/0029-5515/53/4/043004.
Lässer R, et al. (2007) Structural materials for DEMO: The EU development, strategy, testing and modelling. *Fusion Engineering and Design* 82(5–14): 511–520. https://doi.org/10.1016/j.fusengdes.2007.06.031.
Lawson JD (1957) Some Criteria for a Power Producing Thermonuclear Reactor. *Proceedings of the Physical Society. Section B* 70(1): 6–10. https://doi.org/10.1088/0370-1301/70/1/303.
Lazzaro E, et al. (2020) Rocket effect on dust particles in the tokamak {SOL}. *Physica Scripta* 95(5): 55605. https://doi.org/10.1088/1402-4896/ab5ab2.
Lehnen M, et al. (2015) Disruptions in ITER and strategies for their control and mitigation. *Journal of Nuclear Materials* 463: 39–48. https://doi.org/10.1016/j.jnucmat.2014.10.075.
Leipold F, et al. (2016) Cleaning of first mirrors in ITER by means of radio frequency discharges. *Review of Scientific Instruments* 87(11): 8–11. https://doi.org/10.1063/1.4962055.
Levchuk D, et al. (2004) Deuterium permeation through Eurofer and α-alumina coated Eurofer. *Journal of Nuclear Materials* 328(2): 103–106. https://doi.org/10.1016/j.jnucmat.2004.03.008.
Levchuk D, et al. (2007) Erbium oxide as a new promising tritium permeation barrier. *Journal of Nuclear Materials* 367–370: 1033–1037. https://doi.org/10.1016/j.jnucmat.2007.03.183.
Lindau R, et al. (2005) Present development status of EUROFER and ODS-EUROFER for application in blanket concepts. *Fusion Engineering and Design* 75–79: 989–996. https://doi.org/10.1016/j.fusengdes.2005.06.186.
Linke J, et al. (2019) Challenges for plasma-facing components in nuclear fusion. *Matter and Radiation at Extremes* 4(5): 56201. https://doi.org/10.1063/1.5090100.
Litnovsky A, De Temmerman G, et al. (2005a) Direct comparative test of single crystal and polycrystalline diagnostic mirrors exposed in TEXTOR in erosion conditions. In: *32nd EPS Conference on Plasma Physics 2005, EPS 2005, Held with the 8th International Workshop on Fast Ignition of Fusion Targets - Europhysics Conference Abstracts* .
Litnovsky A, Philipps V, et al. (2005b) Experimental investigations of castellated monoblock structures in TEXTOR. *Journal of Nuclear Materials* 337–339(1–3). https://doi.org/10.1016/j.jnucmat.2004.09.064. SPEC. ISS.
Litnovsky A, Philipps V, Kirschner A, et al. (2007a) Carbon transport, deposition and fuel accumulation in castellated structures exposed in TEXTOR. *Journal of Nuclear Materials* 367–370B. https://doi.org/10.1016/j.jnucmat.2007.04.029. SPEC. ISS.
Litnovsky A, Philipps V, Wienhold P, et al. (2007b) Castellated structures for ITER: The influence of the shape of castellation on the impurity deposition and fuel accumulation in gaps. *Physica Scripta*. https://doi.org/10.1088/0031-8949/2007/T128/009.
Litnovsky A, De Temmerman G, et al. (2007c) Investigations of single crystal and polycrystalline metal mirrors under erosion conditions in TEXTOR. *Fusion Engineering and Design* 82(2): 123–132. https://doi.org/10.1016/j.fusengdes.2006.07.095.

Litnovsky A, et al. (2008) First tests of diagnostic mirrors in a tokamak divertor: An overview of experiments in DIII-D. *Fusion Engineering and Design* 83(1). https://doi.org/10.1016/j.fusengdes.2007.06.042.

Litnovsky A, et al. (2009) Castellated structures for ITER: Differences of impurity deposition and fuel accumulation in the toroidal and poloidal gaps. *Journal of Nuclear Materials* 386–388(C). https://doi.org/10.1016/j.jnucmat.2008.12.231.

Litnovsky A, et al. (2010) Mirrors for ITER diagnostics: New R&D developments, assessment of the mirror lifetime and impact of the mirror failure on ITER performance. In: Proceedings of the 23rd IAEA FEC Conference, Vienna: International Atomic Energy Agency Daejeon, South Korea, October 2010. TR/P1-05. Available at: https://www-pub.iaea.org/mtcd/meetings/PDFplus/2010/cn180/cn180_papers/itr_p1-05.pdf.

Litnovsky A, Laengner M, et al. (2011a) Development of in situ cleaning techniques for diagnostic mirrors in ITER. *Fusion Engineering and Design* 86(9–11): 1780. https://doi.org/10.1016/j.fusengdes.2010.11.033.

Litnovsky A, Philipps V, et al. (2011b) Overview of material migration and mixing, fuel retention and cleaning of ITER-like castellated structures in TEXTOR. *Journal of Nuclear Materials* 415(1). https://doi.org/10.1016/j.jnucmat.2010.12.018.

Litnovsky A, et al. (2013) Dust investigations in TEXTOR: Impact of dust on plasma-wall interactions and on plasma performance. *Journal of Nuclear Materials* 438. https://doi.org/10.1016/j.jnucmat.2013.01.020.

Litnovsky A, et al. (2015) Studies of protection and recovery techniques of diagnostic mirrors for ITER. *Nuclear Fusion* 55(9): 093015. https://doi.org/10.1088/0029-5515/55/9/093015.

Litnovsky A, Wegener T, Klein F, Linsmeier C, Rasinski M, Kreter A, Tan X, Schmitz J, Mao Y, et al. (2017a) Advanced smart tungsten alloys for a future fusion power plant. *Plasma Physics and Controlled Fusion* 59(6). https://doi.org/10.1088/1361-6587/aa6948.

Litnovsky A, Krasikov Y, et al. (2017b) First direct comparative test of single crystal rhodium and molybdenum mirrors for ITER diagnostics. *Fusion Engineering and Design* 123. https://doi.org/10.1016/j.fusengdes.2017.03.053.

Litnovsky A, Wegener T, Klein F, Linsmeier C, Rasinski M, Kreter A, Tan X, Schmitz J, Coenen JWW, et al. (2017c) New oxidation-resistant tungsten alloys for use in the nuclear fusion reactors. *Physica Scripta*. https://doi.org/10.1088/1402-4896/aa81f5.

Litnovsky A, Wegener T, Klein F, Linsmeier C, Rasinski M, Kreter A, Unterberg B, et al. (2017d) Smart alloys for a future fusion power plant: First studies under stationary plasma load and in accidental conditions. *Nuclear Materials and Energy* 12. https://doi.org/10.1016/j.nme.2016.11.015.

Litnovsky A, Voitsenya VS, et al. (2019a) Diagnostic mirrors for ITER: Research in the frame of International Tokamak Physics Activity. *Nuclear Fusion* 59(6). https://doi.org/10.1088/1741-4326/ab1446.

Litnovsky A, Peng J, et al. (2019b) Optimization of single crystal mirrors for ITER diagnostics. *Fusion Engineering and Design* 146: 1450–1453. https://doi.org/10.1016/j.fusengdes.2019.02.102.

Litnovsky A, et al. (2020) Smart Tungsten-based Alloys for a First Wall of DEMO. *Fusion Engineering and Design* 159: 111742. https://doi.org/10.1016/j.fusengdes.2020.111742.

Livshits AI, Notkin ME, and Samartsev AA (1990) Physico-chemical origin of superpermeability — Large-scale effects of surface chemistry on "hot" hydrogen permeation and absorption in metals. *Journal of Nuclear Materials* 170(1): 79–94. https://doi.org/10.1016/0022-3115(90)90329-L.

Loarte A (2006) Chaos cuts ELMs down to size. *Nature Physics* 2(6): 369–370. https://doi.org/10.1038/nphys331.

Loarte A, et al. (2007) Chapter 4: Power and particle control. *Nuclear Fusion* 47(6). https://doi.org/10.1088/0029-5515/47/6/S04.

Loarte A, et al. (2015) MHD stability of the ITER pedestal and SOL plasma and its influence on the heat flux width. *Journal of Nuclear Materials* 463: 401–405. https://doi.org/10.1016/j.jnucmat.2014.11.122.

López-Ruiz P, et al. (2011) Self-passivating bulk tungsten-based alloys manufactured by powder metallurgy. *Physica Scripta* T145: 014018. https://doi.org/10.1088/0031-8949/2011/T145/014018.

Lyublinski IE, et al. (2016) Selection of materials for tokamak plasma facing elements based on a liquid tin capillary pore system. *Journal of Physics: Conference Series* 748(1). https://doi.org/10.1088/1742-6596/748/1/012014.

Lyublinsky IE, Vertkov AV, and Evtikhin VA (2007) Physical-chemical basis of lithium use in liquid metal systems of fusion reactor. *Problems of Atomic Science and Technology Series Thermonuclear Fusion* 30: 13.

Maier H, et al. (2019) Deuterium retention in tungsten based materials for fusion applications. *Nuclear Materials and Energy* 18: 245–249. https://doi.org/10.1016/j.nme.2018.12.032.

Maisonnier D (2005) *Final report of the European Fusion Power Plant Conceptual Study (PPCS).* Garching: EFDA. EFDA(05)-27/4.10.

Malang S and Mattas R (1995) Comparison of lithium and the eutectic lead-lithium alloy, two candidate liquid metal breeder materials for self-cooled blankets. *Fusion Engineering and Design* 27(C): 399–406. https://doi.org/10.1016/0920-3796(95)90151-5.

Manhard A, Balden M, and von Toussaint U (2017) Blister formation on rough and technical tungsten surfaces exposed to deuterium plasma. *Nuclear Fusion* 57(12): 126012. https://doi.org/10.1088/1741-4326/aa82c8.

Mao Y, et al. (2018) Influence of the interface strength on the mechanical properties of discontinuous tungsten fiber-reinforced tungsten composites produced by field assisted sintering technology. *Composites Part A: Applied Science and Manufacturing*. https://doi.org/10.1016/j.compositesa.2018.01.022.

Mao Y, Coenen JW, et al. (2019a) Fracture behavior of random distributed short tungsten fiber-reinforced tungsten composites. *Nuclear Fusion*. https://doi.org/10.1088/1741-4326/ab25b0.

Mao Y, Chen C, et al. (2019b) On the nature of carbon embrittlement of tungsten fibers during powder metallurgical processes. *Fusion Engineering and Design*. https://doi.org/10.1016/j.fusengdes.2019.05.033.

Mao Y, et al. (2020) Development of tungsten fiber-reinforced tungsten with a porous matrix. *Physica Scripta* T171: 14030. https://doi.org/10.1088/1402-4896/ab482e.

Markelj S, et al. (2013) Study of thermal hydrogen atom interaction with undamaged and self-damaged tungsten. *Journal of Nuclear Materials* 438: 1027–1031. https://doi.org/10.1016/j.jnucmat.2013.01.224.

Marot L, et al. (2007) Rhodium coated mirrors deposited by magnetron sputtering for fusion applications. *Review of Scientific Instruments* 78(10). https://doi.org/10.1063/1.2800779.

Martin AJ and Ellis GC (1963) *The ductility problem in beryllium. The metallurgy of beryllium.* London: Chapman and Hall.

Martynenko YV and Nagel' MY (2012) Model of fuzz formation on a tungsten surface. *Plasma Physics Reports* 38(12): 996–999. https://doi.org/10.1134/S1063780X12110074.

Matthews GF (2005) Material migration in divertor tokamaks. *Journal of Nuclear Materials* 337–339(1–3): 1–9. https://doi.org/10.1016/j.jnucmat.2004.10.075. SPEC. ISS.

Matthews GF, et al. (2007) Overview of the ITER-like wall project. *Physica Scripta* T128: 137–143. https://doi.org/10.1088/0031-8949/2007/T128/027.

Matthews GF, et al. (2016) Melt damage to the JET ITER-like wall and divertor. *Physica Scripta* T167: 14070. https://doi.org/10.1088/0031-8949/t167/1/014070.

Matveev D, et al. (2014) Estimation of the contribution of gaps to tritium retention in the divertor of ITER. *Physica Scripta* T159: 014063. https://doi.org/10.1088/0031-8949/2014/T159/014063.

Matveeva M, et al. (2010) Material choice for first ITER mirrors under erosion conditions. In: 37th EPS Conference on Plasma Physics 2010, EPS.

Mayer M, et al. (2009) Tungsten erosion and redeposition in the all-tungsten divertor of ASDEX upgrade. *Physica Scripta, T* T138: 1–17. https://doi.org/10.1088/0031-8949/2009/T138/014039.

Mazzitelli G, et al. (2011) FTU results with a liquid lithium limiter. *Nuclear Fusion* 51(7): 4–11. https://doi.org/10.1088/0029-5515/51/7/073006.

Mech BV, Haasz AA, and Davis JW (1998) Model for the chemical erosion of graphite due to low-energy$H+$ and $D+$ impact. *Journal of Applied Physics* 84(3): 1655–1669. https://doi.org/10.1063/1.368235.

Merola M, Wu CH, and EU ITER Participating Team (2004) Development of Carbon Materials and Plasma Facing Components for {ITER}. *Physica Scripta* T111(1): 152. https://doi.org/10.1238/physica.topical.111a00152.

Miquel JL, Lion C, and Vivini P (2016) The laser mega-joule: LMJ & PETAL status and program overview. *Journal of Physics: Conference Series* 688(1). https://doi.org/10.1088/1742-6596/688/1/012067.
Mirnov SV, et al. (2006) Experiments with lithium limiter on T-11M tokamak and applications of the lithium capillary-pore system in future fusion reactor devices. *Plasma Physics and Controlled Fusion* 48(6): 821–837. https://doi.org/10.1088/0741-3335/48/6/009.
Missirlian M, et al. (2014) The WEST project: Current status of the ITER-like tungsten divertor. *Fusion Engineering and Design* 89(7): 1048–1053. https://doi.org/10.1016/j.fusengdes.2014.01.050.
Miyamoto M, et al. (2009) Observations of suppressed retention and blistering for tungsten exposed to deuterium-helium mixture plasmas. *Nuclear Fusion* 49(6). https://doi.org/10.1088/0029-5515/49/6/065035.
Moreau R, Bréchet Y, and Maniguet L (2011) Eurofer corrosion by the flow of the eutectic alloy Pb-Li in the presence of a strong magnetic field. *Fusion Engineering and Design* 86(1): 106–120. https://doi.org/10.1016/j.fusengdes.2010.08.050.
Morgan TW, et al. (2018) Liquid metals as a divertor plasma-facing material explored using the pilot-PSI and Magnum-PSI linear devices. *Plasma Physics and Controlled Fusion* 60(1): 14025. https://doi.org/10.1088/1361-6587/aa86cd.
Morgan TW, et al. (2020) ITER monoblock performance under lifetime loading conditions in Magnum-PSI. *Physica Scripta* T171: 14065. https://doi.org/10.1088/1402-4896/ab66df.
Morozov DK, Baronova EO, and Senichenkov IY (2007) Impurity radiation from a tokamak plasma. *Plasma Physics Reports* 33(11): 906–922. https://doi.org/10.1134/S1063780X07110037.
Moser L, et al. (2015) Plasma cleaning of ITER First Mirrors in magnetic field. *Journal of Nuclear Materials* 463: 940–943. https://doi.org/10.1016/j.jnucmat.2014.11.087.
Möslang A, et al. (2005) Towards reduced activation structural materials data for fusion {DEMO} reactors. *Nuclear Fusion* 45(7): 649–655. https://doi.org/10.1088/0029-5515/45/7/013.
Mukhin EE, Razdobarin GT, Semenov VV, et al. (2008a) Perspectives of use of diagnostic mirrors with transparent protection layer in burning plasma experiments. In: *AIP Conference Proceedings* https://doi.org/10.1063/1.2905100.
Mukhin EE, Razdobarin GT, Kochergin MM, et al. (2008b) Thomson scattering diagnostic systems in the ITER divertor. *Instruments and Experimental Techniques* 51(2): 220–225. https://doi.org/10.1134/S0020441208020115.
Mukhin EE, et al. (2009) Progress in the development of deposition prevention and cleaning techniques of in-vessel optics in ITER. *Nuclear Fusion* 49(8). https://doi.org/10.1088/0029-5515/49/8/085032.
Mukhin EE, et al. (2012) First mirrors in ITER: Material choice and deposition prevention/cleaning techniques. *Nuclear Fusion* 52(1). https://doi.org/10.1088/0029-5515/52/1/013017.
Muller AV, et al. (2017) Melt infiltrated tungsten–copper composites as advanced heat sink materials for plasma facing components of future nuclear fusion devices. *Fusion Engineering and Design* 124: 455–459. https://doi.org/10.1016/j.fusengdes.2017.01.042.
Müller AV, et al. (2019) Additive manufacturing of pure tungsten by means of selective laser beam melting with substrate preheating temperatures up to 1000°C. *Nuclear Materials and Energy* 19: 184–188. https://doi.org/10.1016/j.nme.2019.02.034.
Muroga T (2012) Ceramic coatings as electrical insulators in fusion blankets. *Comprehensive Nuclear Materials* 4: 691–699. https://doi.org/10.1016/B978-0-08-056033-5.00125-7.
Muroga T, et al. (2014) Present status of vanadium alloys for fusion applications. *Journal of Nuclear Materials* 455(1–3): 263–268. https://doi.org/10.1016/j.jnucmat.2014.06.025.
Nagayama Y (2009) Liquid lithium divertor system for fusion reactor. *Fusion Engineering and Design* 84(7): 1380–1383. https://doi.org/10.1016/j.fusengdes.2009.02.002.
Nemanič V (2019) Hydrogen permeation barriers: Basic requirements, materials selection, deposition methods, and quality evaluation. *Nuclear Materials and Energy* 19: 451–457. https://doi.org/10.1016/j.nme.2019.04.001.
Neu R, et al. (2009) Ten years of W programme in {ASDEX} Upgrade{\textemdash}challenges and conclusions. *Physica Scripta* T138: 14038. https://doi.org/10.1088/0031-8949/2009/t138/014038.
Nicholas JR, et al. (2018) Development of a heat sink module for a near-term DEMO divertor. *Fusion Engineering and Design* 133: 77–88. https://doi.org/10.1016/j.fusengdes.2018.05.070.
Nogami S, et al. (2020) Tungsten modified by potassium doping and rhenium addition for fusion reactor applications. *Fusion Engineering and Design* 152. https://doi.org/10.1016/j.fusengdes.2019.111445.
Norimatsu T, et al. (2010) Stagnation of ablated metal vapor in laser fusion reactor with liquid wall. In: Proceedings of the 23 IAEA Fusion Energy Conference, Vienna: International Atomic Energy Agency IFE/P6-21. Available at: https://inis.iaea.org/collection/NCLCollectionStore/_Public/43/033/43033110.pdf?r=1&r=1.
Norimatsu T, et al. (2017) Conceptual design and issues of the laser inertial fusion test (LIFT) reactor—Targets and chamber systems. *Nuclear Fusion* 57: 116040. https://doi.org/10.1088/1741-4326/aa7f07.
Norreys P (2021) In: Greenspan E and Campbell DJ (eds.) *This Encyclopedia*. Elsevier B.V.
Nygren RE and Tabarés FL (2016) Liquid surfaces for fusion plasma facing components—A critical review. Part I: Physics and PSI. *Nuclear Materials and Energy* 9: 6–21. https://doi.org/10.1016/j.nme.2016.08.008.
Ono M, et al. (2017) Liquid lithium applications for solving challenging fusion reactor issues and NSTX-U contributions. *Fusion Engineering and Design* 117: 124–129. https://doi.org/10.1016/j.fusengdes.2016.06.060.
Orsitto FP, et al. (2016) Diagnostics and control for the steady state and pulsed tokamak DEMO. *Nuclear Fusion* 56(2). https://doi.org/10.1088/0029-5515/56/2/026009.
Pégourié B, et al. (2013) Deuterium inventory in Tore Supra: Coupled carbon-deuterium balance. *Journal of Nuclear Materials* 438. https://doi.org/10.1016/j.jnucmat.2013.01.019.
Peng J, et al. (2018) Sputtering tests of single crystal molybdenum and rhodium mirrors at high ion fluence for in situ plasma cleaning of first mirrors in ITER. *Fusion Engineering and Design* 128: 107–112. https://doi.org/10.1016/j.fusengdes.2018.01.061.
Perlado JM, et al. (2010) Chamber responses and Safety and Fusion Technology in HiPER facility. In *Proceedings of the 23rd IAEA FEC Conference*, Daejeon, South Korea, October 2010, IFE/1-5. Vienna: International Atomic Energy Agency.
Perlado JM, et al. (2012) Approach to power plant physics and technology in laser fusion energy systems under repetitive operation. In: *Proceedings of the 24th IAEA Fusion energy conference* 5. IFE-1.5.
Perlado JM, et al. (2018) Thermo-mechanical and atomistic assessment of first wall and optics in non-protective chamber in inertial fusion energy. In: 28th International Atomic Energy Agency Fusion Energy Conference, Vienna: International Atomic Energy Agency October 2018, Ahmedabad, India. IEF/1-4. Available at: https://conferences.iaea.org/event/151/contributions/6091/.
Perrault D (2016) Safety issues to be taken into account in designing future nuclear fusion facilities. *Fusion Engineering and Design* 109–111: 1733–1738. https://doi.org/10.1016/j.fusengdes.2015.10.012.
Peterson BJ, et al. (2008) Development of imaging bolometers for magnetic fusion reactors (invited). *Review of Scientific Instruments* 79(10): 10E301. https://doi.org/10.1063/1.2988822.
Petti DA, et al. (2006) ARIES-AT safety design and analysis. *Fusion Engineering and Design* 80(1–4): 111–137. https://doi.org/10.1016/j.fusengdes.2005.06.351.
Philipps V, et al. (2003) Chemical erosion behaviour of carbon materials in fusion devices. *Journal of Nuclear Materials* 313–316: 354–359. https://doi.org/10.1016/S0022-3115(02)01344-2.
Philipps V, et al. (2010) Overview of the JET ITER-like wall project. *Fusion Engineering and Design* 85(7–9): 1581–1586. https://doi.org/10.1016/j.fusengdes.2010.04.048.
Pint BA, Moser JL, and Tortorelli PF (2007) Investigation of Pb-Li compatibility issues for the dual coolant blanket concept. *Journal of Nuclear Materials* 367–370B: 1150–1154. https://doi.org/10.1016/j.jnucmat.2007.03.206. SPEC. ISS.

Pintsuk G, et al. (2010) Interlaboratory test on thermophysical properties of the ITER grade heat sink material copper–chromium–zirconium. *International Journal of Thermophysics* 31(11): 2147–2158. https://doi.org/10.1007/s10765-010-0857-y.

Pisarev A, et al. (2006) Hydrogen permeation through membranes with rough surface. *AIP Conference Proceedings* 837: 238. https://doi.org/10.1063/1.2213079.

Pitts RA, et al. (2011) Physics basis and design of the ITER plasma-facing components. *Journal of Nuclear Materials* 415(1): S957–S964. https://doi.org/10.1016/j.jnucmat.2011.01.114.

Pitts RA, et al. (2019) Physics basis for the first ITER tungsten divertor. *Nuclear Materials and Energy* 20. https://doi.org/10.1016/j.nme.2019.100696.

Pospieszczyk A, et al. (1999) Chemical erosion in TEXTOR-94. *Physica Scripta* T81: 48–53. https://doi.org/10.1238/physica.topical.081a00048.

Pütterich T, et al. (2010) Calculation and experimental test of the cooling factor of tungsten. *Nuclear Fusion* 50(2): 25012. https://doi.org/10.1088/0029-5515/50/2/025012.

Rapp J, et al. (2002) ELM mitigation by nitrogen seeding in the JET gas box divertor. *Plasma Physics and Controlled Fusion* 44(6): 639–652. https://doi.org/10.1088/0741-3335/44/6/302.

Ratynskaia S, et al. (2013) Migration of tungsten dust in tokamaks: Role of dust-wall collisions. *Nuclear Fusion* 53(12). https://doi.org/10.1088/0029-5515/53/12/123002.

Reiser J, et al. (2017) Ductilisation of tungsten (W): Tungsten laminated composites. *International Journal of Refractory Metals and Hard Materials* 69: 66–109. https://doi.org/10.1016/j.ijrmhm.2017.07.013.

Richou M, et al. (2017) Realization of high heat flux tungsten monoblock type target with graded interlayer for application to {DEMO} divertor. *Physica Scripta* T170: 14022. https://doi.org/10.1088/1402-4896/aa8b02.

Richou M, et al. (2020) Performance assessment of thick W/Cu graded interlayer for DEMO divertor target. *Fusion Engineering and Design* 157: 111610. https://doi.org/10.1016/j.fusengdes.2020.111610.

Riesch J, et al. (2014) Enhanced toughness and stable crack propagation in a novel tungsten fibre-reinforced tungsten composite produced by chemical vapour infiltration. *Physica Scripta* T159: 014031. https://doi.org/10.1088/0031-8949/2014/T159/014031.

Rieth M, et al. (2019) Behavior of tungsten under irradiation and plasma interaction. *Journal of Nuclear Materials* 519: 334–368. https://doi.org/10.1016/j.jnucmat.2019.03.035.

Rigal E, Bucci P, and Le Marois G (2000) Fabrication of monoblock high heat flux components for ITER divertor upper vertical target using hot isostatic pressing diffusion welding. *Fusion Engineering and Design* 49–50: 317–322. https://doi.org/10.1016/S0920-3796(00)00390-2.

Roccella S, et al. (2020) CPS based liquid metal divertor target for EU-DEMO. *Journal of Fusion Energy* 4. https://doi.org/10.1007/s10894-020-00263-4.

Rogerson JE, Davis J, and Jacobs VL (1977) Oxygen impurity radiation from Tokamak-like plasmas. *Journal of Quantitative Spectroscopy and Radiative Transfer* 17(3): 343–349. https://doi.org/10.1016/0022-4073(77)90114-5.

Rogozhkin SV, et al. (2012) Nanoscale study of ferritic-martensitic steel rusfer EK-181 after various heat treatments. *Inorganic Materials: Applied Research* 3(2): 129–134. https://doi.org/10.1134/S2075113312020141.

Roth J (2005) Review and status of physical sputtering and chemical erosion of plasma facing materials. In: Clark REH and Reiter DH (eds.) *Nuclear Fusion Research: Understanding Plasma-Surface Interactions*, pp. 203–224. Berlin, Heidelberg: Springer Berlin Heidelberg. https://doi.org/10.1007/3-540-27362-X_9.

Roth J, et al. (2004) Flux dependence of carbon chemical erosion by deuterium ions. *Nuclear Fusion* 44(11): 21–25. https://doi.org/10.1088/0029-5515/44/11/L01.

Roth J, et al. (2012) D retention in and out-gassing from BeO on Be Co-deposition of hydrogen with PFM atoms. In: Presented at 11th International Workshop on Hydrogen Isotopes in Fusion Reactor Materials, May 29–31, 2012, Schloss Ringberg, Germany.

Rubel M, et al. (2018) Dust generation in tokamaks: Overview of beryllium and tungsten dust characterisation in JET with the ITER-like wall. *Fusion Engineering and Design* 136: 579–586. https://doi.org/10.1016/j.fusengdes.2018.03.027.

Rudakov DL, et al. (2007) DiMES studies of temperature dependence of carbon erosion and re-deposition in the lower divertor of DIII-D under detachment. *Physica Scripta*. https://doi.org/10.1088/0031-8949/2007/T128/006.

Rudakov DL, Litnovsky A, et al. (2009a) Dust studies in DIII-D and TEXTOR. *Nuclear Fusion* 49(8). https://doi.org/10.1088/0029-5515/49/8/085022.

Rudakov DL, Wong CPC, et al. (2009b) Overview of the recent DiMES and MiMES experiments in DIII-D. *Physica Scripta*. https://doi.org/10.1088/0031-8949/2009/T138/014007.

Ruiz JA, Rivera A, et al. (2011a) Materials research for HiPER laser fusion facilities: Chamber wall, structural material and final optics. *Fusion Science and Technology* 60: 565–569. https://doi.org/10.13182/FST11-A12443.

Ruiz JA, Garoz Gomez D, et al. (2011b) The role of spatial and temporal radiation deposition in inertial fusion chambers: The case of HiPER. *Nuclear Fusion* 51: 53019. https://doi.org/10.1088/0029-5515/51/5/053019.

Ruzic DN, et al. (2017) Flowing liquid lithium plasma-facing components – Physics, technology and system analysis of the LiMIT system. *Nuclear Materials and Energy* 12: 1324–1329. https://doi.org/10.1016/j.nme.2017.06.001.

Ryabtsev S, et al. (2016) Deuterium thermal desorption from vacancy clusters in tungsten. *Nuclear Instruments and Methods in Physics Research Section B: Beam Interactions with Materials and Atoms* 382: 101–104. https://doi.org/10.1016/j.nimb.2016.04.038.

Sagara A, et al. (2014) Helical reactor design FFHR-d1 and c1 for steady-state DEMO. *Fusion Engineering and Design* 89(9–10): 2114–2120. https://doi.org/10.1016/j.fusengdes.2014.02.076.

Schmitz J (2020) *Development of Tungsten Alloy Plasma-Facing Materials for the Fusion Power Plant*. Ghent University and University of Bochum.

Schmitz J, et al. (2018) WCrY smart alloys as advanced plasma-facing materials – Exposure to steady-state pure deuterium plasmas in PSI-2. *Nuclear Materials and Energy* 15. https://doi.org/10.1016/j.nme.2018.05.002.

Schmitz J, et al. (2019) Preferential sputtering induced Cr-Diffusion during plasma exposure of WCrY smart alloys. *Journal of Nuclear Materials* 526. https://doi.org/10.1016/j.jnucmat.2019.151767.

Sergienko G, et al. (2007) Experience with bulk tungsten test-limiters under high heat loads: Melting and melt layer propagation. *Physica Scripta* T128: 81–86. https://doi.org/10.1088/0031-8949/2007/T128/016.

Sethian JD, et al. (2010) The science and technologies for fusion energy with lasers and direct-drive targets. *IEEE Transactions on Plasma Science* 38(4): 690–703. https://doi.org/10.1109/TPS.2009.2037629.

Shalpegin A, et al. (2015) Fast camera observations of injected and intrinsic dust in TEXTOR. *Plasma Physics and Controlled Fusion* 57(12). https://doi.org/10.1088/0741-3335/57/12/125017.

Sharpe JP, Petti DA, and Bartels H-W (2002) A review of dust in fusion devices: Implications for safety and operational performance. *Fusion Engineering and Design* 63–64: 153–163. https://doi.org/10.1016/S0920-3796(02)00191-6.

Sharpe JP, et al. (2005) Characterization of dust collected from NSTX and JT-60U. *Journal of Nuclear Materials* 337–339(1–3): 1000–1004. https://doi.org/10.1016/j.jnucmat.2004.09.058. SPEC. ISS.

Shimada M, et al. (2007) ITER physics basis. Chapter 1: Overview and summary. *Nuclear Fusion* 47(6). https://doi.org/10.1088/0029-5515/47/6/S01.

Shu WM, et al. (2007a) Microstructure dependence of deuterium retention and blistering in the near-surface region of tungsten exposed to high flux deuterium plasmas of 38 eV at 315 K. *Physica Scripta* T128: 96–99. https://doi.org/10.1088/0031-8949/2007/t128/019.

Shu WM, Wakai E, and Yamanishi T (2007b) Blister bursting and deuterium bursting release from tungsten exposed to high fluences of high flux and low energy deuterium plasma. *Nuclear Fusion* 47(3): 201–209. https://doi.org/10.1088/0029-5515/47/3/006.

Skinner CH, et al. (2008) Recent advances on hydrogen retention in ITER's plasma-facing materials: Beryllium, carbon, and tungsten. *Fusion Science and Technology* 54(4): 891–945. https://doi.org/10.13182/FST54-891.

Smirnov RD, et al. (2007) Modelling of dynamics and transport of carbon dust particles in tokamaks. *Plasma Physics and Controlled Fusion* 49(4): 347–371. https://doi.org/10.1088/0741-3335/49/4/001.

Smirnov RD, et al. (2009) On visibility of carbon dust particles in fusion plasmas with fast framing cameras. *Plasma Physics and Controlled Fusion* 51(5): 055017. https://doi.org/10.1088/0741-3335/51/5/055017.

Smolentsev S, et al. (2015) Dual-coolant lead-lithium (DCLL) blanket status and R&D needs. *Fusion Engineering and Design* 100: 44–54. https://doi.org/10.1016/j.fusengdes.2014.12.031.

Snead LL and Ferraris M (2020) Graphite and carbon fiber composite for fusion. In: *Reference Module in Materials Science and Materials Engineering*. Elsevierhttps://doi.org/10.1016/B978-0-12-803581-8.11760-6.

Snead LL, et al. (2007) Handbook of SiC properties for fuel performance modeling. *Journal of Nuclear Materials* 371(1–3): 329–377. https://doi.org/10.1016/j.jnucmat.2007.05.016.

Sorbom BN, et al. (2016) The engineering design of ARC: A compact, highfield, fusion nuclear science facility and demonstration power plant. In: *Proceedings—Symposium on Fusion Engineering* 378–405. https://doi.org/10.1109/SOFE.2015.7482330.

Spitzer L, et al. (1954) *Problems of the Stellarator as a Useful Power Source*. Project Matterhorn Princeton University (PM-S). Available at: https://books.google.es/books?id=tWAEfAEACAAJ.

Stangeby PC (2000) *The Plasma Boundary of Magnetic Fusion Devices*. Bristol and Philadelphia: IOP Publishing.

Stangeby P (2011) The strong effect of gaps on the required shaping of the ITER first wall. *Nuclear Fusion* 51(3): 033008. https://doi.org/10.1088/0029-5515/51/3/033008.

Stieglitz R, Boccaccini LV, and Hesch K (2018) Blankets—Key element of a fusion reactor—Functions, design and present state of development. *Kerntechnik* 83(3): 241–250. https://doi.org/10.3139/124.110923.

Stork D, et al. (2014a) Developing structural, high-heat flux and plasma facing materials for a near-term DEMO fusion power plant: The EU assessment. *Journal of Nuclear Materials* 455(1–3): 277–291. https://doi.org/10.1016/j.jnucmat.2014.06.014.

Stork D, et al. (2014b) Materials R&D for a timely DEMO: Key findings and recommendations of the EU roadmap materials assessment Group. *Fusion Engineering and Design* 1586–1594. https://doi.org/10.1016/j.fusengdes.2013.11.007.

Suttrop W, et al. (2018) Experimental conditions to suppress edge localised modes by magnetic perturbations in the ASDEX Upgrade tokamak. *Nuclear Fusion* 58(9), aace93. https://doi.org/10.1088/1741-4326/aace93.

Sykes A, et al. (2018) Compact fusion energy based on the spherical tokamak. *Nuclear Fusion* 58(1). https://doi.org/10.1088/1741-4326/aa8c8d.

Tanabe T, et al. (2005) Tritium retention in the gap between the plasma-facing carbon tiles used in D-T discharge phase in JET and TFTR. *Fusion Science and Technology* 48(1): 577–580. https://doi.org/10.13182/FST05-A991.

Tanigawa H, et al. (2017) Development of benchmark reduced activation ferritic/martensitic steels for fusion energy applications. *Nuclear Fusion* 57(9): 92004. https://doi.org/10.1088/1741-4326/57/9/092004.

Tanigawa H, et al. (2011) Technical issues related to the development of reduced-activation ferritic/martensitic steels as structural materials for a fusion blanket system. *Fusion Engineering and Design* 86(9–11): 2549–2552. https://doi.org/10.1016/j.fusengdes.2011.04.047.

Tassone A, et al. (2018) Recent progress in the WCLL breeding blanket design for the DEMO fusion reactor. *IEEE Transactions on Plasma Science* 46(5). https://doi.org/10.1109/TPS.2017.2786046.

Taylor N (2021) In: Greenspan E and Campbell DJ (eds.) *This Encyclopedia*. Elsevier B.V.

Terra A, et al. (2019) Micro-structured tungsten: An advanced plasma-facing material. *Nuclear Materials and Energy* 19: 7–12.

Tokitani M, et al. (2017) Initial growth phase of W-fuzz formation in ultra-long pulse helium discharge in LHD. *Nuclear Materials and Energy* 12: 1358–1362. https://doi.org/10.1016/j.nme.2016.11.023.

Tokitani M, Masuzaki S, and Murase T (2019) Demonstration of suppression of dust generation and partial reduction of the hydrogen retention by tungsten coated graphite divertor tiles in LHD. *Nuclear Materials and Energy* 18: 23–28. https://doi.org/10.1016/j.nme.2018.11.023.

Tolias P, et al. (2016) Dust remobilization in fusion plasmas under steady state conditions. *Plasma Physics and Controlled Fusion* 58(2). https://doi.org/10.1088/0741-3335/58/2/025009.

Tomastik C, Werner W, and Störi H (2005) Oxidation of beryllium—A scanning Auger investigation. *Nuclear Fusion* 4580. https://doi.org/10.1088/0029-5515/45/9/005.

Tortorelli PF (1992) Dissolution kinetics of steels exposed in lead-lithium and lithium environments. *Journal of Nuclear Materials* 191–194(B): 965–969. https://doi.org/10.1016/0022-3115(92)90617-T.

Trufanov D, Marenkov E, and Krasheninnikov S (2015) The role of the adatom diffusion in the Tungsten fuzz growth. *Physics Procedia* 71: 20–24.

Tsitrone E, et al. (2011) Multi machine scaling of fuel retention in 4 carbon dominated tokamaks. *Journal of Nuclear Materials* 415. https://doi.org/10.1016/j.jnucmat.2011.01.132.

Tsui Y, Surrey E, and Hampshire D (2016) 'Soldered joints—An essential component of demountable high temperature superconducting fusion magnets. *Superconductor Science and Technology* 29(7). https://doi.org/10.1088/0953-2048/29/7/075005.

Tyumentsev AN, et al. (2012) Microstructure of EK-181 ferritic-martensitic steel after heat treatment under various conditions. *Technical Physics* 57(1): 48–54. https://doi.org/10.1134/S1063784212010264.

Ueda Y, et al. (2011) Exposure of tungsten nano-structure to TEXTOR edge plasma. *Journal of Nuclear Materials* S92. https://doi.org/10.1016/j.jnucmat.2010.08.019.

Ueda Y, et al. (2014) Research status and issues of tungsten plasma facing materials for ITER and beyond. *Fusion Engineering and Design* 89(7–8): 901–906. https://doi.org/10.1016/j.fusengdes.2014.02.078.

Van der Schaaf B, et al. (2003) The development of EUROFER reduced activation steel. *Fusion Engineering and Design* 69(1–4): 197–203. https://doi.org/10.1016/S0920-3796(03)00337-5. SPEC.

Van Dorsselaere JP, et al. (2012) Progress of IRSN R&D on ITER safety assessment. *Journal of Fusion Energy* 31(4): 405–410. https://doi.org/10.1007/s10894-011-9485-1.

Vayakis G, et al. (2008) Chapter 12: Generic diagnostic issues for a burning plasma experiment. *Fusion Science and Technology* 53(2): 699–750. https://doi.org/10.13182/FST08-A1684.

Vila R and Hodgson ER (2009) A TIEMF model and some implications for ITER magnetic diagnostics. *Fusion Engineering and Design* 84(7–11): 1937–1940. https://doi.org/10.1016/j.fusengdes.2009.01.025.

Voitsenya VSS and Litnovsky A (2009) Investigations of mirrors for ITER diagnostics in modern fusion devices. *Plasma Devices and Operations* 17(4): 309–318. https://doi.org/10.1080/10519990903157399.

Voitsenya V, et al. (2001) Diagnostic first mirrors for burning plasma experiments (invited). *Review of Scientific Instruments* 72(1): 475–482. https://doi.org/10.1063/1.1310580.

Von Keudell A and Jacob W (1996) Growth and erosion of hydrocarbon films investigated by in situ ellipsometry. *Journal of Applied Physics* 79(2): 1092–1098. https://doi.org/10.1063/1.360796.

Wade M (2021) In: Greenspan E and Campbell DJ (eds.) *This Encyclopedia*. Elsevier B.V.

Wagner F, et al. (1982) Regime of improved confinement and high beta in neutral-beam-heated divertor discharges of the ASDEX Tokamak. *Physical Review Letters* 49(19): 1408–1412. https://doi.org/10.1103/PhysRevLett.49.1408.

Walker CI, et al. (2005) ITER diagnostics: Maintenance and commissioning in the hot cell test bed. *Fusion Engineering and Design* 74(1–4): 685–690. https://doi.org/10.1016/j.fusengdes.2005.06.243.

Wang L, et al. (2020) Contrasting roles of Laves_Cr2Nb precipitates on the creep properties of novel CuCrNbZr alloys. *Materials Science and Engineering A* 779: 139110. https://doi.org/10.1016/j.msea.2020.139110.

Wauters T, et al. (2020) 'Wall conditioning in fusion devices with superconducting coils. *Plasma Physics and Controlled Fusion* 62(3): 34002. https://doi.org/10.1088/1361-6587/ab5ad0.

Weber T, et al. (2013) Functionally graded vacuum plasma sprayed and magnetron sputtered tungsten/EUROFER97 interlayers for joints in helium-cooled divertor components. *Journal of Nuclear Materials* 436(1): 29–39. https://doi.org/10.1016/j.jnucmat.2013.01.286.

Wegener T, et al. (2016) Development of yttrium-containing self-passivating tungsten alloys for future fusion power plants. *Nuclear Materials and Energy* 9. https://doi.org/10.1016/j.nme.2016.07.011.
Wegener T, et al. (2017) Development and analyses of self-passivating tungsten alloys for DEMO accidental conditions. *Fusion Engineering and Design* 124. https://doi.org/10.1016/j.fusengdes.2017.03.072.
Wenninger R, et al. (2017) 'The DEMO wall load challenge. *Nuclear Fusion* 57(4): 46002. https://doi.org/10.1088/1741-4326/aa4fb4.
Wesson J and Campbell DJ (2011) *Tokamaks*. OUP Oxford. International Series of Monogr. Available at: https://books.google.de/books?id=BH9vx-iDI74C.
Wienhold P, et al. (1999) Investigation of erosion and deposition on wall components of TEXTOR-94. *Physica Scripta, T* 81: 19–24. https://doi.org/10.1238/physica.topical.081a00019.
Wienhold P, et al. (2003) Short and long range transport of materials eroded from wall components in fusion devices. *Journal of Nuclear Materials* 313–316: 311–320. https://doi.org/10.1016/S0022-3115(02)01347-8.
Winter J (1996) Wall conditioning in fusion devices and its influence on plasma performance. *Plasma Physics and Controlled Fusion* 38(9): 1503–1542. https://doi.org/10.1088/0741-3335/38/9/001.
Winter J (1998) Dust in fusion devices—Experimental evidence, possible sources and consequences. *Plasma Physics and Controlled Fusion* 40(6): 1201–1210. https://doi.org/10.1088/0741-3335/40/6/022.
Winter J (2004) Dust in fusion devices—A multi-faceted problem connecting high- and low-temperature plasma physics. *Plasma Physics and Controlled Fusion* 46(12 B): 583–592. https://doi.org/10.1088/0741-3335/46/12B/047.
Wong CPC, et al. (2007) Divertor and midplane materials evaluation system in DIII-D. *Journal of Nuclear Materials* 363–365(1–3). https://doi.org/10.1016/j.jnucmat.2007.01.121.
Wong CPC, et al. (2013) Plasma Surface Interaction (PSI) studies at DIII-D. In: 2013 IEEE 25th Symposium on Fusion Engineering, SOFE 2013, IEEEhttps://doi.org/10.1109/SOFE.2013.6635337.
Wu Y, et al. (2016) Identification of safety gaps for fusion demonstration reactors. *Nature Energy* 1(12). https://doi.org/10.1038/nenergy.2016.154.
Yamada H (2021) In: Greenspan E and Campbell DJ (eds.) *This Encyclopedia*. Elsevier B.V.
Yamagiwa M, et al. (2011) Helium bubble formation on tungsten in dependence of fabrication method. *Journal of Nuclear Materials* 417(1): 499–503. https://doi.org/10.1016/j.jnucmat.2011.02.007.
Yan R, et al. (2018) Plasma cleaning of ITER edge Thomson scattering mock-up mirror in the EAST tokamak. *Nuclear Fusion* 58: 026008. https://doi.org/10.1088/1741-4326/aa96b8.
Yang Q, et al. (2017) Development of the flowing liquid lithium limiter for EAST tokamak. *Fusion Engineering and Design* 124: 179–182. https://doi.org/10.1016/j.fusengdes.2017.04.063.
You JH (2015) Copper matrix composites as heat sink materials for water-cooled divertor target. *Nuclear Materials and Energy* 5: 7–18. https://doi.org/10.1016/j.nme.2015.10.001.
Zakharov LE (2019) On a burning plasma low recycling regime with P DT = 23-26 MW, Q DT = 5-7 in a JET-like tokamak. *Nuclear Fusion* 59(9): ab246b. https://doi.org/10.1088/1741-4326/ab246b.
Zammuto I, et al. (2018) Cracks avoidance with a modified solid tungsten divertor in ASDEX Upgrade. *Fusion Engineering and Design* 136: 1052–1057. https://doi.org/10.1016/j.fusengdes.2018.04.066.
Zhang Y, Tucker GJ, and Trelewicz JR (2017) Stress-assisted grain growth in nanocrystalline metals: Grain boundary mediated mechanisms and stabilization through alloying. *Acta Materialia* 131: 39–47. https://doi.org/10.1016/j.actamat.2017.03.060.
Zinkle SJ (1994) Ceramics Radiation Effects Issues For Iter. *Plasma Devices and Operations* 3: 139–149. https://doi.org/10.1080/10519999408201810.
Zinkle SJ (2005) Advanced materials for fusion technology. *Fusion Engineering and Design* 74(1–4): 31–40. https://doi.org/10.1016/j.fusengdes.2005.08.008.
Zinkle SJ (2016) 'Applicability of copper alloys for DEMO high heat flux components. *Physica Scripta* T167: 14004. https://doi.org/10.1088/0031-8949/2015/T167/014004.
Zinkle SJ and Busby JT (2009) Structural materials for fission & fusion energy. *Materials Today* 12(11): 12–19. https://doi.org/10.1016/S1369-7021(09)70294-9.
Zinkle SJ and Möslang A (2013) Evaluation of irradiation facility options for fusion materials research and development. *Fusion Engineering and Design* 88(6–8): 472–482. https://doi.org/10.1016/j.fusengdes.2013.02.081.
Zinkle SJ, et al. (2013) Multimodal options for materials research to advance the basis for fusion energy in the ITER era. *Nuclear Fusion* 53(10). https://doi.org/10.1088/0029-5515/53/10/104024.
Zinkle SJ, et al. (2017) Development of next generation tempered and ODS reduced activation ferritic/martensitic steels for fusion energy applications. *Nuclear Fusion* 57(9): 92005. https://doi.org/10.1088/1741-4326/57/9/092005.
Zinkle SJ, Tanigawa H, and Wirth BD (2019) In: Odette GR and Zinkle SJ (eds.) *Chapter 5—Radiation and Thermomechanical Degradation Effects in Reactor Structural Alloys*, pp. 163–210. Boston: Elsevier. https://doi.org/10.1016/B978-0-12-397046-6.00005-8.
Zlobinski M, et al. (2019) Fuel Retention Diagnostic Setup (FREDIS) for desorption of gases from beryllium and tritium containing samples. *Fusion Engineering and Design* 146: 1176–1180. https://doi.org/10.1016/j.fusengdes.2019.02.035.
Zmitko M, et al. (2017) The European ITER Test Blanket Modules: EUROFER97 material and TBM's fabrication technologies development and qualification. *Fusion Engineering and Design* 124: 767–773. https://doi.org/10.1016/j.fusengdes.2017.04.051.
Zohm H (2021) In: Greenspan E and Campbell DJ (eds.) *This Encyclopedia*. Elsevier B.V.